Future Energy
Open Access Journal
ISSN 2832-0328

May 2026| Volume 05 | Issue 02 | Pages 47-72

Journal homepage: https://fupubco.com/fuen

https://doi.org/10.55670/fpll.fuen.5.2.5

Future Publishing LLC

Review

A comprehensive review of recent advances in biomass pyrolysis: feedstock characteristics, thermal decomposition mechanism, temperature, heating rate, residence time, and particle size on product distribution

Ashraful Islam[1], Mehedi Hasan Kazol[1], Mizanur Rahman[1]*, Abdullah Al Rifat[1], Nurul Amin[2]

[1]Department of Mechanical Engineering, Chittagong University of Engineering and Technology, Chattogram-4349, Bangladesh
[2]Chittagong Water Supply and Sewerage Authority, CWASA, Bangladesh

ARTICLE INFO

Article history:
Received 20 December 2025
Received in revised form
27 February 2026
Accepted 04 April 2026

Keywords:
Biomass pyrolysis, Reaction mechanisms, Kinetic modeling, Bio-oil and biochar, Process optimization

*Corresponding author
Email address:
mmrahman_me@cuet.ac.bd

DOI: 10.55670/fpll.fuen.5.2.5

ABSTRACT

Biomass pyrolysis is a promising thermochemical conversion pathway for producing renewable fuels, value-added chemicals, and carbon-based materials from sustainable feedstocks. However, the complex and highly sensitive nature of pyrolysis reactions, governed by biomass composition, operating conditions, and reactor design, continues to challenge predictive control and large-scale deployment. This review provides a comprehensive and critical synthesis of recent advances in biomass pyrolysis, with particular emphasis on feedstock characteristics; the thermal decomposition mechanisms of cellulose, hemicellulose, and lignin; and the influence of key operational parameters, such as temperature, heating rate, residence time, and particle size, on product distribution. Special attention is given to reaction intermediates and pathways identified through advanced analytical techniques, including Py-GC/MS, TG-FTIR, two-dimensional photoionization mass spectrometry, and complementary molecular-level simulations such as density functional theory and reactive molecular dynamics. By systematically integrating experimental observations with mechanistic insights, this review highlights current limitations, including the lack of unified kinetic models, weak coupling between experiments and simulations, and insufficient investigation of high-temperature pyrolysis regimes above 800 °C. Emerging opportunities for data-driven and machine-learning-assisted kinetic modeling are also discussed as a pathway to address biomass heterogeneity and complex reaction networks. The findings presented herein aim to support the development of predictive pyrolysis models, optimized reactor design, and the sustainable valorization of biomass within future bioenergy and biorefinery systems.

1. Introduction

A promising method, biomass pyrolysis, uses organic materials such as wood, crop residues, and solid waste to produce green fuels such as gas, biochar, and bio-oil [1]. Biofuels and important intermediary chemicals can be produced through biomass pyrolysis, a thermochemical conversion process. Biomass pyrolysis technology still faces a number of difficulties despite its enormous potential, including the unpredictability of pyrolysis products, tar treatment and utilization, and the lack of uniform guidelines for the use of bio-oil [2]. Biomass is one of the most promising substitutes for fossil fuels because of its abundant supply and near-zero carbon emissions. Renewable energy can be enhanced using lignocellulosic biomass, mainly comprising cellulose in the range of 15.2% (pistachio shell)-67.0% (cotton stalk), hemicellulose from 5.2% (sunflower) to 38.2% (pistachio shell), and lignin from 6.5% (rye)-53.5% (walnut shell) [3]. During combustion, the formation of low-melting-

point compounds, such as potassium chloride and potassium sulphate, is primarily responsible for biomass ash-related problems; thus, it has become a major concern in the biomass energy industry. So far, these problems include slagging, fouling, bed agglomeration, and corrosion [4]. To address these problems, it is essential to understand the mechanisms of ash deposition and the preventive strategies. When local biomass and waste are used, co-combustion of biomass with fossil fuels is an efficient way to lower greenhouse gas emissions from the heat and power generation industry. Existing fossil-fuel boilers can be inexpensively modified to accommodate up to 20% biomass [5]. Co-combustion can greatly lower nitrogen oxides without raising carbon monoxide emissions, but its long-term potential may be limited by the ultimate phase-out of coal power stations and issues, including feed type, moisture content, and combustor design, that require ongoing optimization. Biomass is compacted into solid briquettes during the physical conversion process, thereby increasing its energy density and facilitating storage and transportation [6]. Anaerobic digestion and syngas fermentation are two biochemical conversion techniques that break down non-woody organic materials in the absence of oxygen, producing stable gases such as carbon dioxide and methane [7]. In addition, because nitrogen is less expensive than argon and helium, it is the most widely used carrier gas. Unlike photolysis, which uses heat and light to break down a chemical molecule. During pyrolysis, the biomass organic matrix decomposed into solid, liquid, and non-condensable gas products. It has a fast biomass conversion rate, which is especially valuable for char and liquid production [8]. Several additional processes occur in the system concurrently with pyrolysis. The temperature and residence-time distributions of gases, oils, and chars affect reactions [9].

Biomass, which includes wood and forestry leftovers, agricultural crops and their byproducts, municipal solid trash, and food waste, is a diverse and renewable source of organic matter. Additionally, it comprises post-consumer wood, aquatic biomass including plants and algae, animal waste, and byproducts from wood and agri-food industries [10]. Because of the wide range of feedstock options available for energy recovery and chemical valorization, biomass serves as a substitute for traditional fossil fuels [11]. The EU is expected to continue and even increase its supply of sustainable biomass through 2050, as shown in Figure 1, with major contributions coming from organic waste streams, forest biomass, and agricultural residues. While bio-waste makes up a very small portion of the total volume, agricultural and forestry biomass are the main contributors to the total biomass potential and are an important source of biomass availability for energy production. Depending on legislative changes, sustainability standards, and technological breakthroughs, the amount of biomass available for bioenergy is projected to range from 520 to 860 million dry tons by 2050 [10]. These projections underscore the urgent need for effective thermochemical technologies to meet these goals while also contributing to circular, decarbonized economies in which research and innovation drive enhanced conversion efficiencies and reduced environmental impacts.

Its increasing availability underscores the need to study and utilize the diverse energy services biomass can provide across a variety of sectors and at multiple scales. Biomass is a flexible energy source used in many applications, including electricity generation, district and home heating, transportation fuels, and process heat in industrial processes [12].

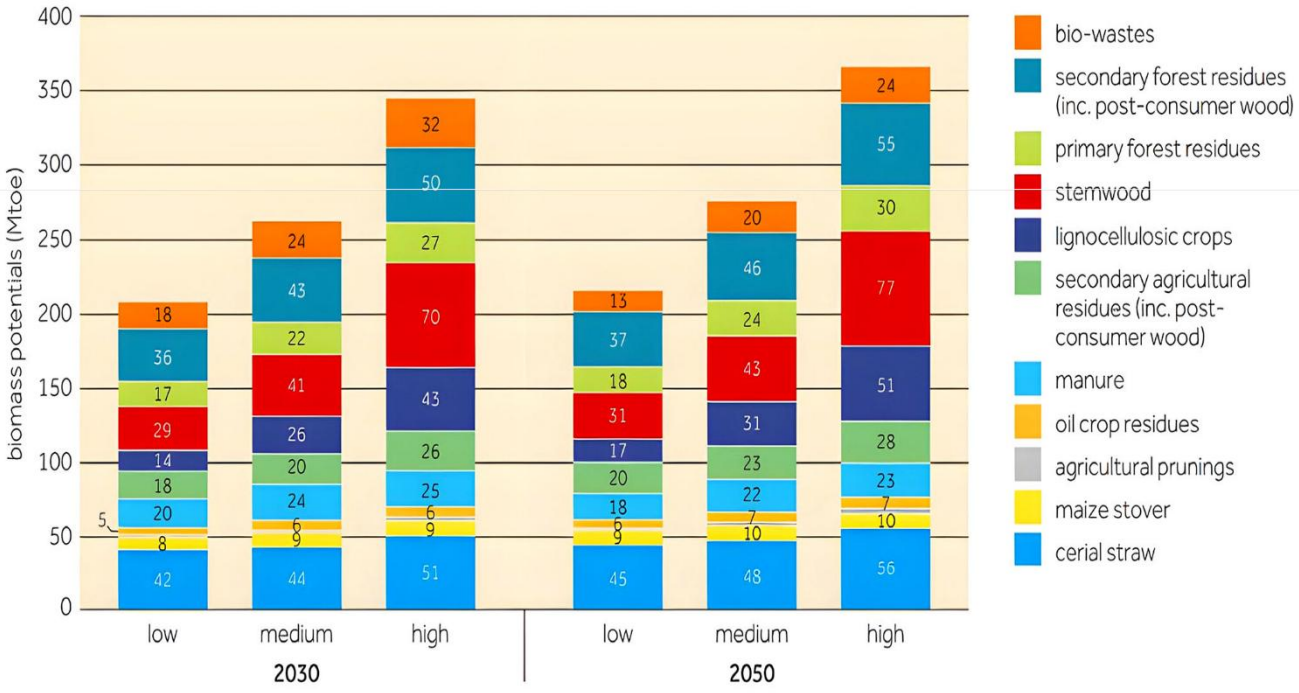

Figure 1. Potential for bioenergy from sustainable biomass in 2030 to 2050 [10]

Biomass pyrolysis is generally categorized as slow, fast, or flash pyrolysis based on the heating rate because it is an extremely sensitive thermochemical process to reaction parameters. Temperature, heating rate, residence time, and particle size are important process variables that significantly impact yield and product quality [13]. Among these, the heating rate governs the reaction pathways, while temperature primarily influences the product distribution. Heavy tar is the main product of biomass decomposition at low temperatures (<300°C), although both production and quality of bio-oil are maximized at medium temperatures (400-550°C). Gas generation is increased at high temperatures (>600°C), because of increased secondary cracking. The increased energy input encourages further reactions by facilitating the disintegration of chemical bonds and biomass structure [14]. By reducing heat and mass transport constraints, preventing tar cracking and repolymerization, and enhancing product selectivity, especially at medium temperatures under rapid heating conditions, the heating rate, a crucial kinetic element, increases the yield of bio-oil [15].

For effective pyrolysis and precise control over product distribution and characteristics, optimizing temperature and heating rate is essential. Plant cell walls include lignin, a highly cross-linked, irregular phenolic polymer that functions as a natural "glue" providing biomass with structural stability and biological resilience. Lignin is the most resistant component of lignocellulosic biomass because of its hydrophobicity and chemical recalcitrance; this makes it an ideal starting point for making biochar with generally high solid yields. These alterations are accompanied by the progressive removal of oxygen-containing functional groups (such as -COOH, -OH) and the development of aromatic structures, both of which are very temperature-dependent [16]. As a result, pyrolysis temperatures between 500 and 800°C are often considered ideal for balancing material quality and yield.

Despite their potential to uncover deeper Mechanisms of structural evolution and enable high-value applications, research at higher temperatures (>800°C) is still limited due to technical difficulties. High-temperature pyrolysis (HTP, 800-1000°C) promotes substantial aromatization, defect correction, and the formation of graphite-like domains in biochar, compared with traditional low- and medium-temperature pyrolysis (300-700°C). While HTP biochar has better-structured carbon frameworks and improved physicochemical stability, low-temperature biochar retains numerous oxygenated functional groups and exhibits limited conductivity [17].

In this study, we reviewed process parameters, analytical techniques, and identified intermediates in biomass pyrolysis (Figure 2). Understanding biomass pyrolysis requires a comprehensive evaluation of both the operating conditions governing thermal decomposition and the analytical approaches used to detect and characterize the intermediates formed during the process. Key process parameters-including types of pyrolysis, reactor configuration, feed rate, operating temperature, heating rate, residence time, particle size, biomass types and compositions, and carrier gas flow conditions-collectively influence the yield distribution and chemical pathways leading to liquid, gas, and solid products. In parallel, advancements in analytical techniques have enabled detailed identification of transient intermediates across various product phases, offering insights into dominant reaction mechanisms and the formation of major chemical families, including acids, aldehydes, ketones, furans, phenolics, anhydro-sugars, and light hydrocarbons. However, despite significant progress, the literature remains fragmented with limited integration between process parameter variations and the corresponding intermediate species detected through analytical platforms.

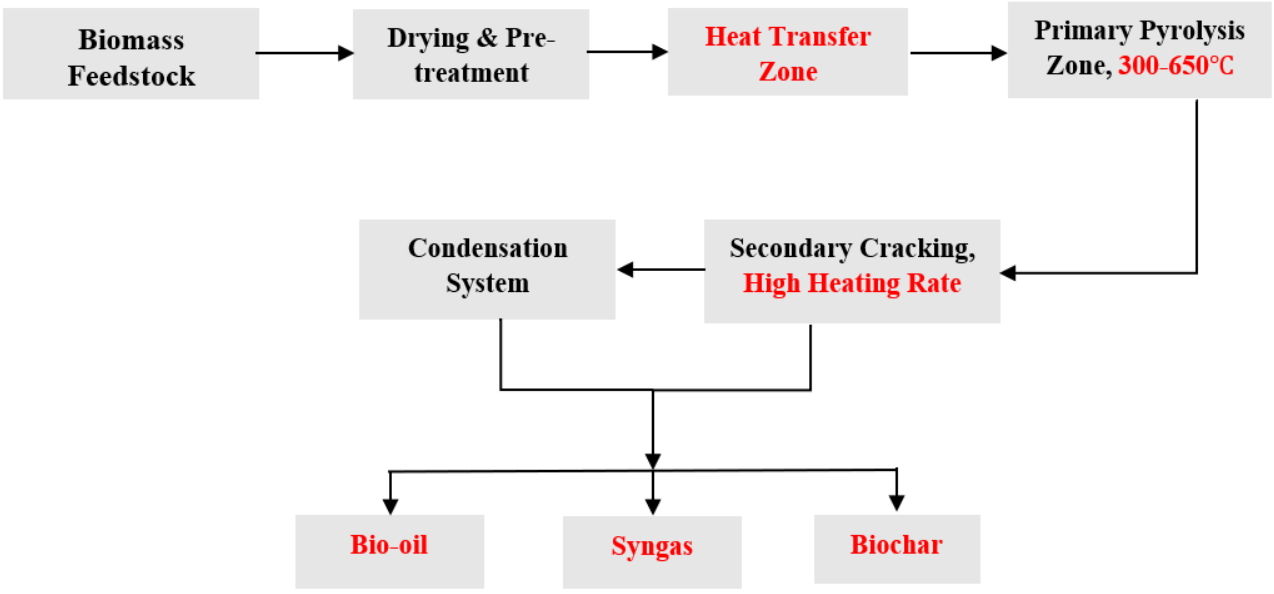

Figure 2. Process flow diagram of biomass pyrolysis

Therefore, this review consolidates existing knowledge by systematically comparing process conditions and their impact on pyrolysis intermediates, highlighting the role of analytical methodologies in elucidating reaction pathways. This approach aims to provide a clearer mechanistic understanding to support optimized reactor design, improved product selectivity, and the advancement of biomass-to-biofuel and biomaterials technologies.

2. Comprehensive overview of biomass thermal decomposition

The main raw materials utilized in biomass pyrolysis are wood chips or agricultural waste, which are components of lignocellulosic biomass [18]. The distribution of pyrolysis products from different types of biomasses is the focus of most mechanistic research on real biomass pyrolysis processes, or attempts to identify the corresponding kinetic parameters based on macroscopic thermal breakdown processes [19]. An essential first step in understanding the basic pyrolysis mechanism is to examine the reaction processes of each main component of biomass. The three primary components of lignocellulosic biomass-cellulose, hemicellulose, and lignin, dominate and compose the biomass's main structure, even when it contains a minor amount of ash and extracts, especially in wood biomass, where the contents can reach 90% [20,21]. Among the main components, cellulose is the most basic polysaccharide, a linear polymer. It is made up of several glucose basic units joined by β-1,4-glycosidic linkages [22]. The microscopic structural alterations, reaction pathways, and creation mechanism of several common products, such as levoglucosan, have been the primary focus of recent research on the cellulose pyrolysis mechanism [23].

Ali et al. [24] claimed that more furans were generated during the pyrolysis of glucose than during the pyrolysis of glucose than during the pyrolysis of cellulose. Li et al. [25] used a combination of DFT calculations and PY-GC experiments to investigate cellulose as a model compound. Their results showed that the reducing and non-reducing ends of the cellulose chain first generated distinct chain ends and dehydrated units through cleavage of β-1,4-glycosidic linkages. As seen in Figure 3, these chain ends and dehydrated units subsequently generated various pyrolytic products via various reaction routes. In the pyrolysis investigation of microcrystalline cellulose, Li et al. [26] also integrated in situ DRIFT with 2D-PICS analysis. They discovered that the breakdown of cellulose's main chain came before the dehydration of free hydroxyls, with hydrogen-bond networks being broken first.

The heat stability of the C-O bond between the glucopyranose ring and hydroxyl is superior to that of the C-O bond between the glucopyranose ring and the glycosidic bond. Larger cellulose pyrolysis reaction systems have been used in several studies, necessitating the use of different, more suitable analysis techniques. Reactive force field molecular dynamics, or ReaxFF MD, is a bond order-based molecular dynamics technique that was recently applied to biomass pyrolysis due to its lower computational resource requirements. Zeng et al. [27] used ReaxFF MD to study the generation and evaluation of main pyrolysis products such as glycolaldehyde and levoglucosan of the big cellulose molecule (C_{2160} H_{3612} O_{1800}) at temperatures between 500 and 1400 K. they discovered that whereas levoglucosan synthesis rapidly decreased as the temperature rose, high temperatures encouraged the development of glycolaldehyde.

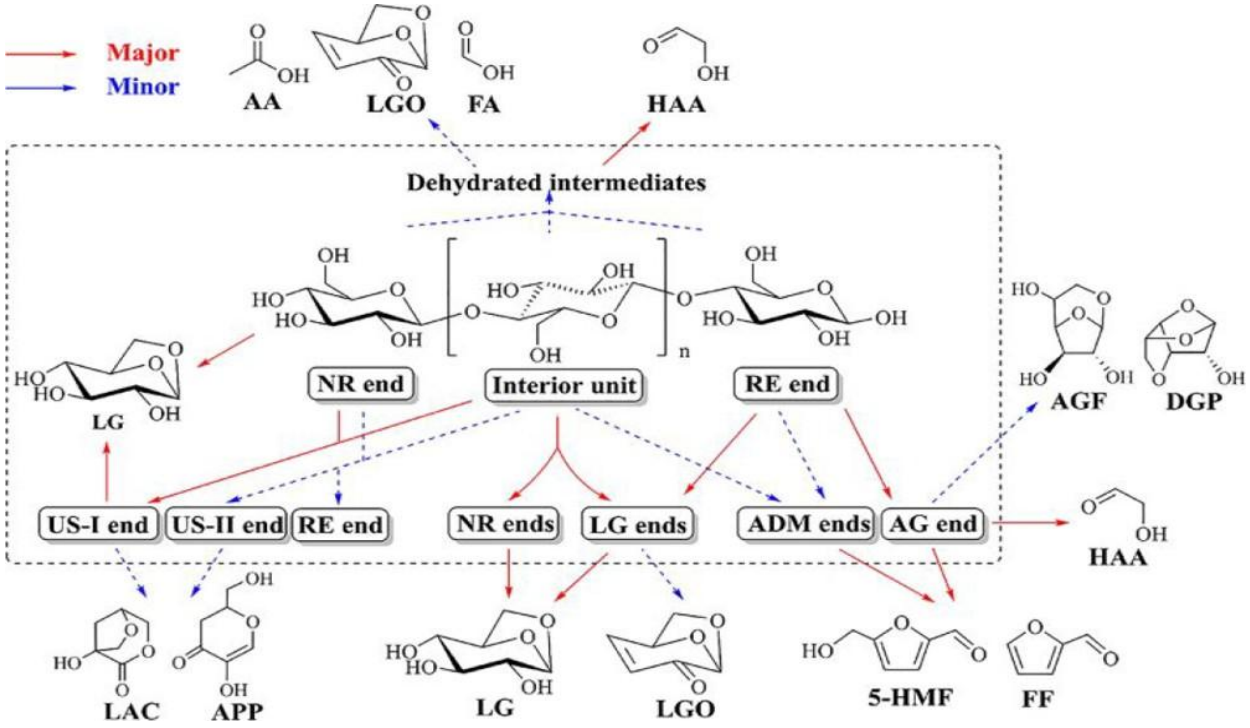

Figure 3. Basic schematic illustrating the mechanism of cellulose pyrolysis [25]

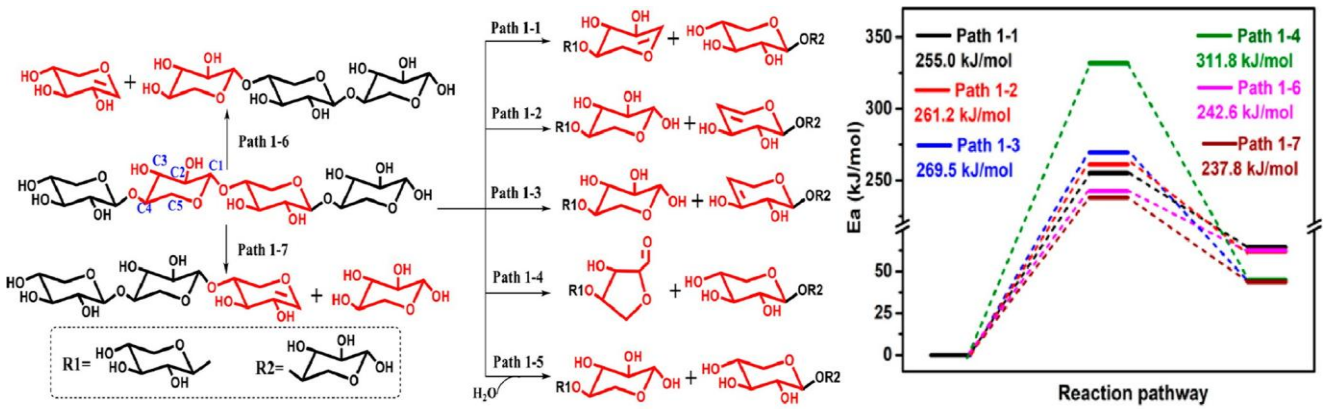

Figure 4. Simplified mechanism schematic highlighting glycosidic bond scission occurring during hemicellulose pyrolysis [29]

For FF formation, the total energy barrier was 259.8 KJ/mol. Due to their resemblance to actual hemicellulose, xylo-bios and xylan were also chosen as model compounds in consideration of the glycosidic bond of the main chain of xylan. Zhu and Du [28] used Py-GC/MS and DFT calculations to investigate the pyrolysis mechanism pf xylose, xylobiose and xylan. Because of the glycosidic link, they found that xylose and xylo-biose yielded differing amounts of the main pyrolysis products, particularly 1,4-anhydro-xylopyranose. Xylan;s high degree of polymerization hindered its depolymerization, and its side chains had an impact on the pyrolysis process and product distribution. According to Du et al. [29], a competitive reaction mechanism was responsible for the dissociation of side chains and the disruption of glycosidic bonds in xylan. Figure 4 illustrates the breakdown of glycosidic linkages in the hemicellulose main chain.

Understanding the pyrolysis mechanism of hemicellulose is challenging due to its complex structure. A somewhat comprehensive model of hemicellulose pyrolysis involving intermediates, low-molecular-weight products, and the associated reaction was developed by Yang et al. [30]. Routes and expanded it to include native hemicellulose. According to their model, hemicellulose pyrolysis began with the cleavage of hemicellulose chains, producing monomers such as xylose and anhydroxylose. These monomers were further broken down by subsequent reactions, such as ring opening, dehydration, retro-aldol, and enol-ketone isomerization, to produce pyrolysis products such as furfural, glycolaldehyde, and hydroxyacetone. Using 2D-PICS, Wang et al. [31] investigated the evolution of the functional groups during the first phase of low-temperature pyrolysis of poplar wood lignin. They suggested that some small-molecule volatiles, such as CO and CO_2, would be released as the temperature increased due to the tendency of hydroxyl and hydrocarbon groups to dissolve. As seen in Figure 5, Zhou et al. [32] used ReaxFF MD to simulate the pyrolysis process of softwood lignin polymers. They proposed that cleavage of α -O-4 and β-O-4 bonds, which break down lignin macromolecules, began before the first pyrolysis phase of lignin (the initial phase). Then the temperature rises, and every connection ruptures (the 2nd step).

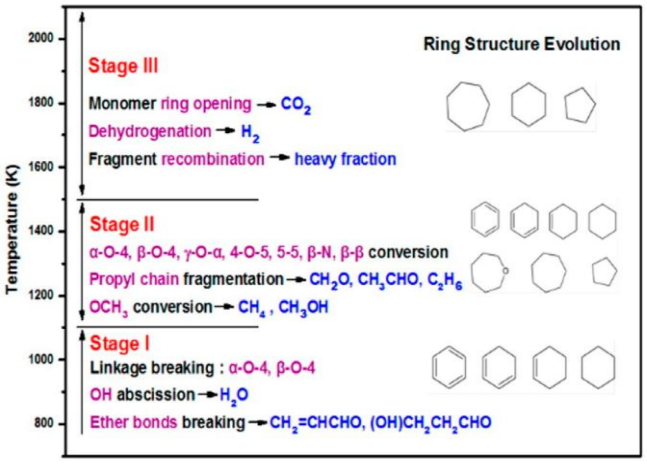

Figure 5. Overview schematic depicting the fundamental steps in lignin pyrolysis [32]

The heavy pyrolytic compounds would next be produced mostly by regrouping 5, 6, or 7-membered aliphatic rings at higher temperatures (3rd phase).

3. Fundamental characteristics of biomass-derived feedstocks and reaction-kinetic models

Understanding the chemical composition of biomass and how each component interacts with selected conversion methods is necessary to address the variability concerns. Extractives are compounds that are soluble in water, such as proteins and non-structural carbohydrates, and soluble in ethanol, such as waxes and chlorophyll. Hemicellulose volatiles can make oil produced by thermochemical methods more acidic, which is associated with increased viscosity during bio-oil storage [33]. Herbaceous feedstocks typically exhibit greater compositional variability than woody biomass and have a higher ash content. Nevertheless, not all characterization techniques yield the same estimates of biomass composition, leading to apparent biomass variability that depends on the techniques used to assess the relevant characteristics [34]. In reviewing biomass characteristics, multiple sources of biomass variability have been comprehensively assessed. Variation in the chemical characteristics of different feedstocks must be accounted for when using multiple feedstocks in a particular conversion

process. Table 1 presents numerous structural evaluations of a variety of biomass samples, using data from the INL database and combining chemical data from earlier assessments. Herbaceous materials have the lowest lignin content, while pine, a softwood, and hybrid poplar, a hardwood, have the highest lignin content. Because of its high energy content, the material's heating value is in the same order as lignin. Before selecting a processing or conversion technique, such a compositional datum is crucial for comprehending the characteristics of the feedstocks. For example, softwoods may be more suited for combustion in energy applications due to their higher lignin concentration. The composition of each feedstock varies greatly (Table 2). When additional, more varied bioenergy feedstocks are taken into account, this issue is made worse. Natural rangeland grasses that are mixed and suitable for fermentation are an excellent illustration of this. Compared to conventional energy crops, these grasses usually require less maintenance and preserve natural habitats, but their inherent high variability may result in lower, highly variable product yields. More C_4 prairie grass energy crops, such as switchgrass, which store more carbon than typical C_3 conservation grassland species are being targeted, resulting in a significant increase in ethanol output per unit area [35].

For each parameter category, the number of samples included in the average is indicated by *n*; the numbers in parentheses denote one standard deviation [36]. While the bark has a higher lignin content and the leaves have a higher extractives concentration, the heartwood contains the majority of the cellulose in woody biomass. However, the leaves and internodes (the concentration between different stalk segments) contain the majority of the extractives in maize stover. Across biomass types, variations in composition by anatomical fraction can also be identified. For instance, different wheat stover fractions might differ by more than 10% in their glucan content, with some fractions being far more susceptible to chemical saccharification. Certain plants are more susceptible to saccharification in maize stover, where the cobs, husks, and leaves react better to simultaneous saccharification and fermentation (SSF) than the stocks, while having similar glucan levels [38]. If the anatomical fractionation can increase a process's profitability by isolating high-value components. The utilization of distiller dried grains with solubles (DDGS) in ethanol production for high-protein animal feed, rather than converting it into fuels or chemicals, demonstrates this [39]. Figure 6 provides an overview of the structure of a typical complex reaction kinetics model used for biomass pyrolysis.

Table 1. Overview of structural composition found in a range of biomass feedstocks

The Parameter	Pine	Hybrid poplar	Switchgrass	Corn stover
Analysis of proximity (wt.%)	n=27	n=19	n=102	n=171
Ash	0.60 (0.3)	1.20 (0.1)	6.80 (4)	7.60 (4.1)
Volatile matter	0.60 (0.3)	1.20 (0.1)	6.80 (4.0)	7.61 (4.1)
Fixed carbon	76.40 (6.9)	84.01 (0.6)	74.90 (6.3)	75.41 (4.8)
(wt.%) Ultimate analysis	17.90 (3.5)	14.80 (0.6)	14.40 (2.2)	14.81 (1.6)
Carbon	n=26	n=19	n=102	n=170
Hydrogen	49.40 (1.7)	50.0 (0.2)	45.50 (3.8)	44.41 (3.6)
Oxygen	6.40 (0.2)	5.91 (0.1)	5.90 (0.3)	5.91 (0.4)
Nitrogen	43.50 (1.6)	42.51 (0.3)	41.6 0(2.4)	42.80 (3.6)
Sulfur	0.20 (0.1)	0.31 (0.1)	0.80 (0.7)	0.60 (0.2)
Chlorine (PPM)	0.00 (0.0)	0.00 (0.0)	0.10 (0.0)	0.10 (0.0)
Higher Heating Value (HHV) (MJ/kg, dry basis)	42 (36)	19	1400	8500 (6200)
Average structural components (dry basis)	19.6 (0.7)	20.2 (0.3)	17.0 (1.0)	17.3 (0.7)
Cellulose	n=9	n=5	n=30	n=23
Hemicellulose	30.91 (5.5)	45.70 (3.1)	34.40 (5.0)	34.60 (3.1)
Lignin	19.31 (1.5)	19.10 (2.1)	25.70 (4.9)	24.60 (4.1)
Extractives	29.01 (2.1)	24.90 (2.6)	16.10 (2.3)	13.90 (1.7)

Table 2. Variation in the composition of woody biomass and corn stover across different anatomical fractions [37]

Structural Elements	Hemicellulose	cellulose	Lignin	Extractives
Woody biomass (wt.%)	-	-	-	-
Entire tree	23.40	51.21	25.41	3.01
Bark	47.01	22.01	31.01	3.30
Twigs	62.30	15.40	22.30	1.61
Leaves	47.20	26.51	26.31	3.72
Corn cob	30.71	35.93	16.45	5.90
Corn leaves	22.78	34.34	14.00	10.55
Corn husk	31.19	37.74	10.53	5.81
Corn internodes	20.04	40.22	17.25	12.30

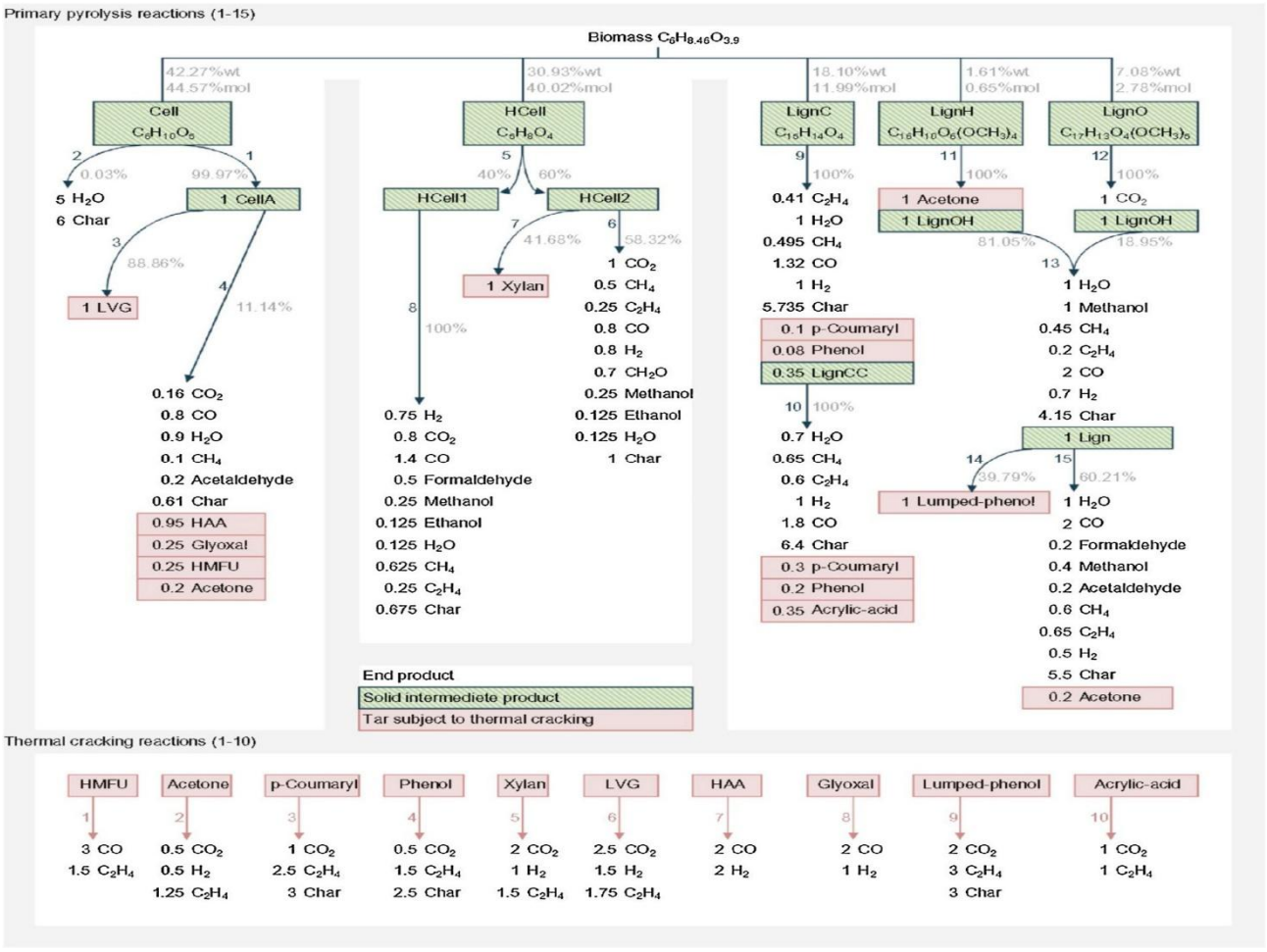

Figure 6. Overview diagram depicting the structure of a typical complex reaction-kinetics model used for biomass pyrolysis [40]

4. Primary operational parameters governing pyrolysis processes

Based on key process variables such as final temperature, heating rate, residence time, feed rate, particle size, feedstock variability, and carrier gas flow, pyrolysis can be divided into several categories. Slow, moderate, rapid, and flash pyrolysis are the most commonly used types. In contrast, other methods, such as microwave-assisted, catalytic, vacuum, or hydro-pyrolysis, remain niche or emerging technologies with little industrial use. As a result, these four basic conventional pyrolysis processes will be the subject of the following sections. Depending on energy requirements and application objectives, these four categories offer flexibility in adjusting product distributions toward syngas, biochar, or bio-oil. It is helpful to remember that the technological readiness levels (TRLs) of pyrolysis processes vary widely depending on reactor design, operating scale, and anticipated products before going over each type separately. With many commercial units in operation and a TRL of 8-9, slow pyrolysis is typically the most developed method in the European environment. With several pilot demonstration-scale facilities, fast pyrolysis, aimed at producing bio-oil, is at TRL 6-8. Particularly in early pilot studies or laboratory research, flash and catalytic pyrolysis continue to operate at lower TRL values (3-5).

The historical focus of each process charcoal for slow pyrolysis, liquid fuels for fast pyrolysis, and high-efficiency gas production or selective chemical synthesis for flash or catalytic pathways is referred to in these differences in maturity [41]. The historical emphasis on rapid pyrolysis, high-efficiency gas production, or selective chemical synthesis via flash or catalytic pathways is reflected in differences in maturity. The discrepancy highlights how process development must be integrated with market and regulatory incentives in order to maximize the value of certain pyrolysis products. Additionally, TRL differences affect investment attractiveness and determine each technology's capacity for scale-up in real-world applications. The primary purpose of slow pyrolysis, also known as carbonization or conventional pyrolysis, is to make biochar. Since the early 20th century, slow pyrolysis-often referred to as the classic type of pyrolysis-has been used in industry. A variety of chemicals, including methanol, ethanol, acetic acid, and carbonaceous residues, were produced in its early applications by subjecting biomass, especially wood, to prolonged heat decomposition, typically lasting up to 24 hours [42]. Intermediate pyrolysis runs at temperatures between 500 and 700°C, with heating rates ranging from 0.4-10°C/s and biomass residence durations of 0.5-40s. This approach is especially appealing for integrated biorefinery

applications that aim to effectively valorize all product fractions since it allows a balanced distribution of solid liquid, and gaseous products. In the context of circular economy models and sustainable waste management, such integrated valorization is essential, particularly in areas that produce significant amounts of agricultural or agro-industrial waste [43]. Fast pyrolysis is regarded as a sophisticated thermochemical conversion technique that was created specifically to increase the output of bio-oil by quick thermal breakdown of biomass under strictly regulated process conditions. Although wider operating windows from 300-1400℃ [44]. Flash pyrolysis is characterized by extraordinarily high temperatures (between 600 and 1400℃) of 1000-2100℃ per second. The quick thermal decomposition of biomass is made possible by extremely short reaction times, which typically range from 0.5-2 seconds [45].

In summary, the key operational parameters of pyrolysis-particularly heating rate, pyrolysis process temperature, residence time, feed rate, particle size, carrier gas flow, feedstock variance, and reactor types-play a critical influence in defining whether a system operates in the slow, intermediate, fast, or flash regime. Slow pyrolysis, defined by low heating rates and lengthy residence times, supports maximal char yield, whilst intermediate conditions yield a balanced product distribution appropriate for flexible downstream applications. Fast pyrolysis, achieved by high heating rates and short vapor residence times, enables rapid depolymerization and secondary cracking, thereby boosting liquid product yields. At the extreme end, flash pyrolysis achieves ultrafast heating and residence times in milliseconds, leading to highly reactive intermediates and dominant vapor-phase products. Collectively, these operating regimes influence the physicochemical environment of biomass breakdown and govern the selectivity, quality, and yield of pyrolysis intermediates and end products. Understanding these interdependent paths and adapting pyrolysis systems for specific energy, chemical, and material uses (Figure 7).

Appendix 1 summarizes an overview of the process factors influencing pyrolysis and co-pyrolysis.

5. Overview of analytical approaches applied in biomass pyrolysis

The process of clarifying a substance's characteristics is referred to as characterization. Spectroscopy, microscopy, calorimetry, light or radiation scattering, chromatography, and gravimetric processes are common methods. To clarify the physical and chemical properties of bio-oil, biochar, and gases generated during pyrolysis, a variety of analytical techniques have been used. Qualitative analytical data require as many analytical techniques as feasible to determine the unequivocal identity of unknowns. On the other hand, meticulous observation, a suitable hypothesis, a methodical experimental design, statistical data analysis, result validation, and repeatable findings guarantee the validity and reliability of quantitative measures. Adequate sample pretreatment is used to ensure this, with the goal of enhancing selectivity and specificity in analysis. A specific component or its class (target analytes) can be determined (enrichment) or eliminated as a result of sample preparation, which reduces background and matrix interferences. All forms of analysis require sample pre-treatment, which is considered extremely labor-intensive. There is a wealth of information in the literature on selecting an effective sample-preparation strategy for instrumental analysis, and modern sample extraction techniques have evolved from traditional solvent- and absorbent-based methods. Samples pre-treatment is commonly followed by derivatization for chromatographic procedures to avoid the detrimental effects of constituents in complex matrices on analytical columns. Derivatization improves the chromatographic properties of labile chemicals and gives thermal stability. Furthermore, it ensures the quality of analytical data by enhancing the sensitivity of detection in specific instrumental tests (e.g., pentaflurobenzyle and silyl methyl are typical derivatives for chromatographic analysis).

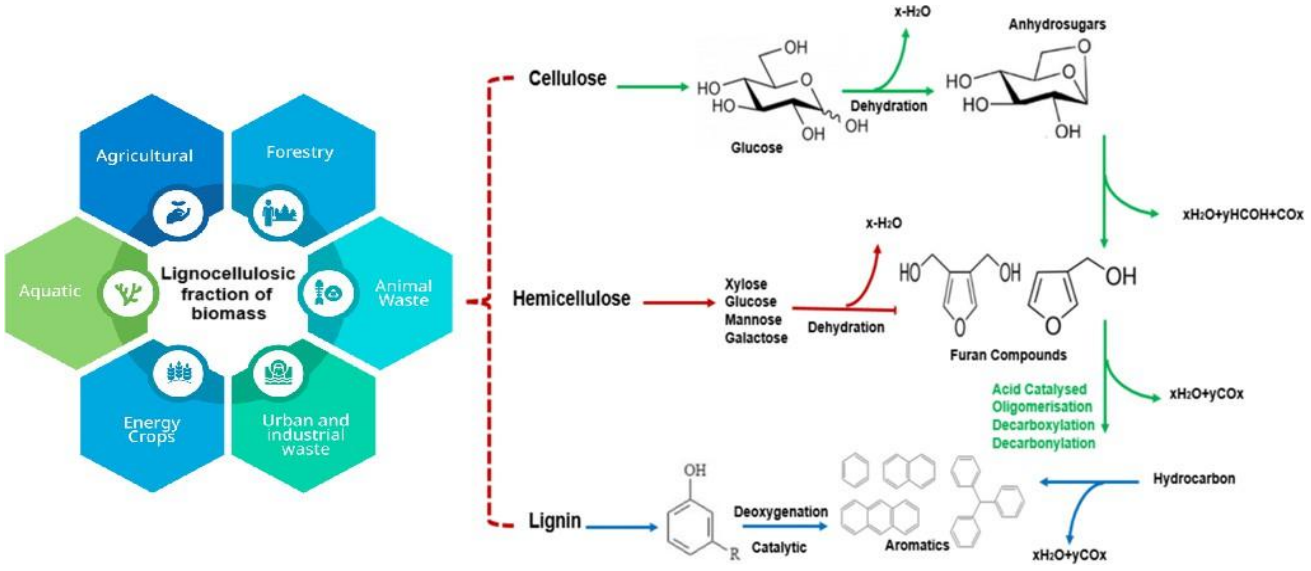

Figure 7. Overview of the reaction routes followed by lignocellulosic fractions in biomass during pyrolysis [46]

Table 3. ASTM methods for assessing the physical properties of pyrolysis oils: a concise summary [143]

Physical Property	ASTM Standard	Evaluation Method
Density	D1298	Method of Hydrometer
	D4052	A digital density gauge
	D369 (withdrawn)	Specific gravity using a pycnometer
Water (%)	D1744 (withdrawn)	Method of Karl Fisher volumetric
	D95	Method of distillation
	E203	The volumetric Karl Fisher method
Ash (%)	D482	Thermogravimetry method
Viscosity	D88	Say-bolt viscosity utilizing a viscometer
	D445	Capillary method through viscometer
	D2170	Liquid flow utilizing calibrated glass capillary method
Flash point	D93	Flash point by specified rate of heating
	D3828	A small-scale cup test where a sample is introduced and an ignition spark is produced
Heating value	D3286 (withdrawn)	The Iso-Peribol Bomb calorimeter's gross calorific value of coal and coke
	D240	Heat of combustion using a Bomb Calorimeter
	D4809	Using a Bomb Calorimeter
Total acid value	D974	Color indicator titration
	D664	Method of potentiometric titration technique
	D3339	Titration of semi-micro color indicator
Pour point	D97	Specific cooling of a hot sample and mobility monitoring of the sample
Elemental analysis	D5373	Estimation of NO_x, CO_2, H_2O (oxidization of sample H, N and C)
	D5291	Identifying the gases that are produced after being converted from the corresponding elements
Volatiles in bio-char	D3175	Gravimetric analysis of weight loss under strictly regulated circumstances
Fixed carbon/ash content of bio-char	D3174	Gravimetry in regulated environment
Sulfur analysis	D4239	SO_x measurement using infrared following sample combustion
	D4294	Method of Energy Dispersive X-ray Fluorescence Spectrometry
	D2622	Method of Wavelength Dispersive X-ray Fluorescence Spectrometry
Surface tension	D971	Interfacial tension is measured by moving a platinum ring from the surface of
Carbon residue	D189	Evaluation of carbon residue using the destructive distillation method
	D4530	Micro-method (gravimetric analysis in an inert nitrogen atmosphere at 500°C)

Numerous investigation reports silyation followed by GC-MS analysis for polar Pyro-oil components (such as alcohols, carboxylic acids, and phenols). There are so many different compounds with different functional groups; pyro-oil analysis is quite similar to petroleum analysis. More than 400 different molecules, including heavy polar compounds, non-polar aliphatic, alicyclic, olefins, aromatics, and oxygenates, are found in bio-oils. The inclusion of macromolecules derived from lignin and cellulose further complicates the analytical setting. Sample preparation techniques cannot be generalized to pyro-oils because the relative concentrations of chemicals vary with several variables (e.g., pyrolysis settings, reactor design, and biomass feedstocks). Table 3 presents the American Society for Testing and Materials (ASTM) methods for assessing the physical properties of pyrolysis oils, a concise summary [143].

6. Output formed during pyrolysis reactions

Lignocellulosic materials are converted by biomass pyrolysis into three main product streams: Bio-oil (Table 4), Non-condensable gases, and Biochar. Temperature, heating rate, and vapor residence time all have a significant impact on the yields of these compounds, which are produced when cellulose, hemicellulose, lignin are thermally broken down in an oxygen-free environment. While the persistent gases are in the creation of syngas or process energy, bio-oil is a complex combination of oxygenated molecules with potential fuel and chemical value. The solid carbonaceous residue is becoming increasingly valuable for use in catalysis, carbon storage, and soil improvement. Optimizing pyrolysis systems and improving downstream upgrading procedures requires an understanding of formal features and the interactions among these product factions. Bio-oil is typically considered a crude product that requires further processing to yield high-quality liquid fuels and chemicals [145]. When used directly in combustion engines, bio-oil produced during biomass pyrolysis typically has a high oxygen and moisture content (15-60%), which reduces its sustainability as a replacement for traditional petroleum fuels [146]. All things considered, biochar is an extremely valuable byproduct of biomass pyrolysis with benefits that go beyond its energy content. Pyrolysis temperature, heating rate, and feedstock characteristics significantly influence the physicochemical features of the product, including aromaticity, porosity, mineral content, and surface functionality (Table 5). These characteristics dictate its applicability for a variety of uses,

such as carbon sequestration, soil amendment, catalysis, adsorption, and electrochemical devices. Targeted process control and engineered alterations are enabling the creation of customized biochar with improved performance as knowledge of the principles underlying biochar formation advances. As a result, biochar is becoming a versatile substance that greatly enhances the sustainability and circularity of thermochemical biomass conversion, while also serving as a stable carbon store (Figure 8). The analytical techniques used in biomass pyrolysis provide crucial insights into the thermal and chemical processes that govern the transformation of lignocellulosic materials. Each of the three methods-spectroscopy, chromatography, and thermos-analysis contributes distinct and complementary data on reaction kinetics, product composition, and structural evolution. The integration of approaches such as FTIR, NMR, GC-MS, TGA, and hyphenated systems (e.g., TGA-FTIR, Py-GC-MS) enhances the resolution with which volatile production, intermediate routes, and solid-phase changes may be characterized.

Table 4. Physiochemical attributes of bio-oil [144]

Property	Value
Sulphur (%)	<0.005
Nitrogen (%)	<0.4
Moisture Content (%)	20-30%
Ash content (%)	0.01-0.1
pH	2 to 3
Density (kg/dm^3)	1.10-1.30
Viscosity (40°C)	15-35
Flash point	40-110
Pour Point (°C)	-9 to -36
Suspended solids (%)	<0.5
Lower Heating Value (LHV) (MJ/kg)	13 to 18

When combined, these technologies provide a more thorough understanding of biomass breakdown behavior, facilitating better process modeling, reactor optimization, and strategic pyrolysis product upgrading. Therefore, the development of effective, commercially feasible thermochemical conversion technologies and a deeper mechanistic understanding will depend on ongoing progress and the coupling of analytical techniques. In spite of having extensive research on biomass pyrolysis, many critical gaps remain that limit the development of predictive, scalable, and optimized conversion technologies. First, the absence of unified reaction-kinetic models remains a major challenge. Most existing kinetic models are developed for specific biomass types, temperature ranges, or reactor configurations, making them difficult to generalize across diverse feedstocks and operating conditions. The strong dependence of reaction pathways on heating rate, residence time, and biomass composition further complicates the development of transferable kinetic frameworks. Second, experimental investigations and numerical studies are weakly integrated. While advanced experimental techniques such as Py-GC/MS, TG-FTIR, and 2D photoionization mass spectrometry have provided valuable insights into pyrolysis intermediates, these datasets are rarely used to validate or refine molecular-level simulations such as density functional theory (DFT) or reactive force field molecular dynamics (ReaxFF MD). As a result, many simulation-based reaction mechanisms lack experimental verification, reducing their reliability for process design and scale-up. Third, high-temperature pyrolysis regimes above 800 °C remain insufficiently explored, despite their relevance for syngas production, hydrogen-rich gas formation, and the synthesis of structurally ordered biochar and carbon materials. Most experimental studies focus on low- to medium-temperature pyrolysis, leaving significant knowledge gaps regarding reaction pathways, intermediate stability, and product evolution under extreme thermal conditions. Appendix 2 presents biomass type, analytical techniques, product phase and chemical families in pyrolysis.

Table 5. Representative properties of biochar produced from different biomass feedstocks

Feedstocks	Composition (%)					
	Carbon	Hydrogen	Nitrogen	Sulfur	Oxygen	Ash
Almond	87.91	2.50	1.11	0.51	7.81	2.81
Bamboo	76.68	1.70	0.58	0.29	5.82	8.71
Beech	73.61	3.41	0.21	-	6.31	-
Iroko	68.41	3.41	0.21	-	15.31	-
Eucalyptus	79.52	2.78	0.18	0.28	-	5.01
Olive	78.69	2.84	0.99	0.033	12.89	-
Banana	48.01	3.21	1.21	0.34	-	23.51
Spruce	72.91	3.31	0.21	-	12.81	-
Switch grass	87.24	2.70	1.34	0	8.74	-
Rice straw	67.89	1.50	1.12	0.28	8.96	-
Grape seeds	84.71	1.31	1.61	0.31	12.11	13.11
Wheat straw	64.28	2.38	0.47	0.31	14.30	-
Miscanthus	44.30	5.73	0.46	-	49.51	8.79
Rice Husk	51.52	2.14	0.46	0.021	9.77	-
Corn cobs	67.70	3.20	0.50	-	9.20	-
Sugarcane	41.31	2.91	0.41	0.11	-	33.81
Corn stover	56.71	1.90	0.76	0.22	-	5.01

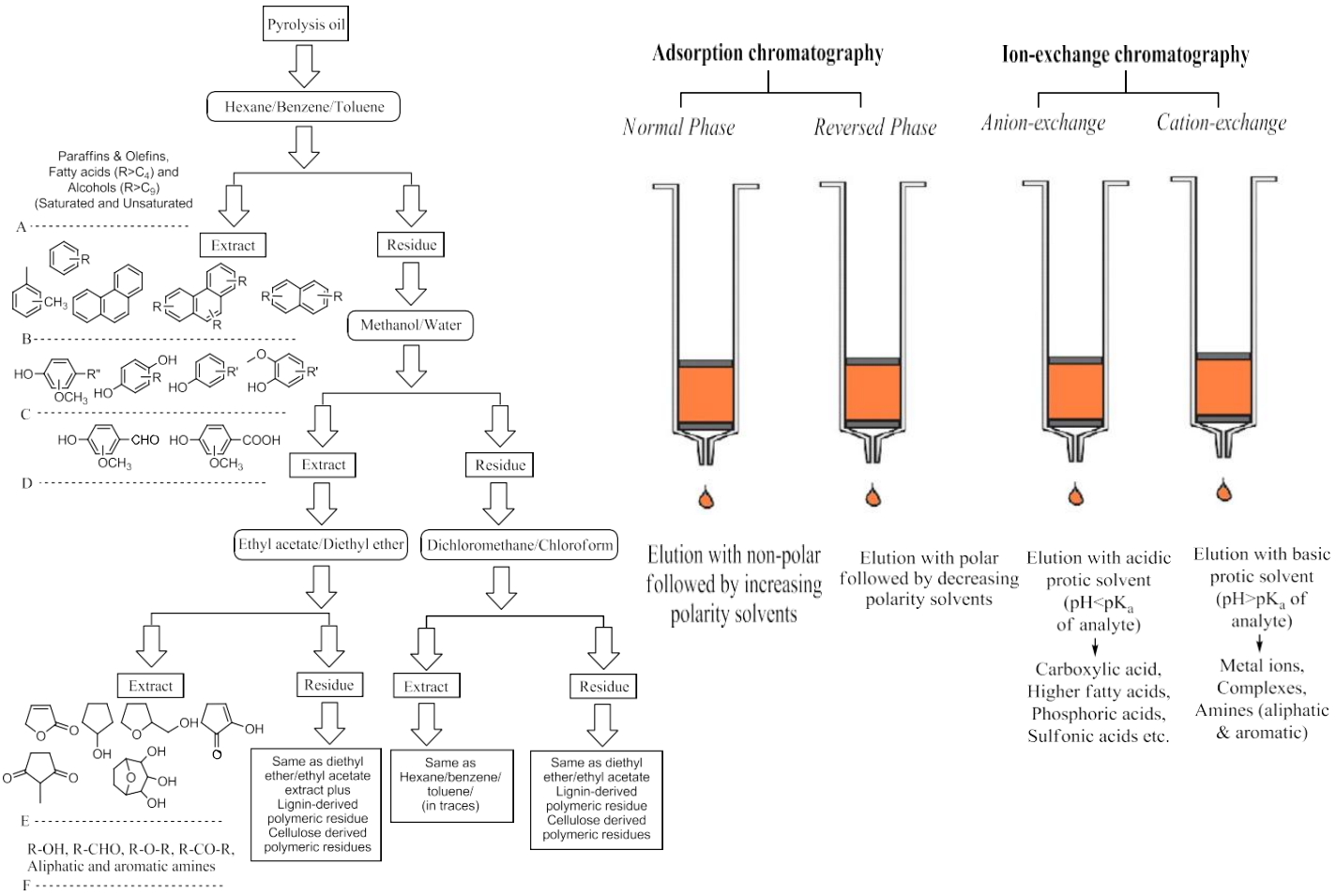

Figure 8. Recommended sample-preparation workflow for pyrolysis oil employing liquid-liquid extraction followed by chromatographic analysis [146]

Finally, the application of data-driven and artificial intelligence-based modeling approaches to biomass pyrolysis remains limited. Given the inherent heterogeneity of biomass and the complexity of pyrolysis reaction networks, traditional mechanistic models often struggle to capture nonlinear interactions between process parameters and product distributions. The lack of integrated experimental databases further restricts the development of machine-learning-assisted kinetic models capable of adaptive prediction and optimization. Addressing these gaps requires a multidisciplinary approach that integrates systematic experimental studies, validated molecular simulations, high-temperature investigations, and data-driven modeling to achieve a comprehensive, predictive understanding of biomass pyrolysis processes.

7. Conclusion

Biomass pyrolysis is a flexible and promising thermochemical process for the sustainable transformation of lignocellulosic resources into biofuels, value-added chemicals, and functional carbon materials. By carefully evaluating feedstock properties, the thermal breakdown mechanisms of cellulose, hemicellulose, and lignin, and the impact of critical operating parameters such as temperature, heating rate, residence time, and particle size on product distribution, this review provided a comprehensive overview of recent developments in biomass pyrolysis. Using complementary molecular-level simulations and sophisticated analytical methods such as Py-GC/MS, TG-FTIR, and two-dimensional photoionization mass spectrometry, special attention was made to identifying chemical intermediates and dominant routes. The results show that the intrinsic variability of biomass and the complex relationship between reaction kinetics and process parameters significantly influence pyrolysis behavior. The lack of unified kinetic models that can capture multi-scale reaction networks, the lack of integration between experimental observations and computational modeling, and the lack of investigation of high-temperature pyrolysis regimes above 800 °C are some of the major challenges that still exist despite the significant progress made in clarifying individual component mechanisms and parameter effects. Predictive control and large-scale pyrolysis system optimization are restricted by these deficiencies. In the future, combining data-driven strategies such as machine-learning-supported kinetic modeling, high-temperature experimental investigations, and sophisticated in situ diagnostics offers a viable approach to addressing reaction complexity and biomass variability. Enhancing product selectivity, process efficiency, and scalability will require a better link between reactor design and mechanistic knowledge. To facilitate the development of next-generation pyrolysis technologies and enable the

sustainable valorization of biomass within future bioenergy and biorefinery frameworks, this review aims to serve as an extensive resource for academics and engineers.

Acknowledgement
The authors are grateful to Chittagong University of Engineering & Technology, Chattogram-4349, Bangladesh, for providing financial support through Research Grant CUET/DRE/2024-25/ME/056.

Ethical issue
The authors are aware of and comply with best practices in publication ethics, specifically concerning authorship (avoidance of guest authorship), dual submission, manipulation of figures, competing interests, and compliance with policies on research ethics. The authors adhere to publication requirements that the submitted work is original and has not been published elsewhere in any language.

Data availability statement
The manuscript contains all the data. However, more data will be available upon request from the corresponding author.

Conflict of interest
The authors declare no potential conflict of interest.

References
[1] A. Bieniek, M. Sieradzka, W. Jerzak, and A. Magdziarz, "Fast pyrolysis of agricultural biomass in drop tube reactor for bio-oil production: Numerical calculations," J. Anal. Appl. Pyrolysis, vol. 176, p. 106241, Nov. 2023, doi: 10.1016/j.jaap.2023.106241.
[2] S. Gao et al., "Assessment of particle shape and size effects on biomass pyrolysis products distribution and reaction kinetics," Appl. Therm. Eng., vol. 271, p. 126334, Jul. 2025, doi: 10.1016/j.applthermaleng.2025.126334.
[3] G. Wang et al., "A Review of Recent Advances in Biomass Pyrolysis," Energy Fuels, vol. 34, no. 12, pp. 15557–15578, Dec. 2020, doi: 10.1021/acs.energyfuels.0c03107.
[4] A. Tshikovhi, T. E. Motaung, A. Tshikovhi, and T. E. Motaung, "Technologies and Innovations for Biomass Energy Production," Sustainability, vol. 15, no. 16, Aug. 2023, doi: 10.3390/su151612121.
[5] X. Hu and M. Gholizadeh, "Biomass pyrolysis: A review of the process development and challenges from initial researches up to the commercialisation stage," J. Energy Chem., vol. 39, pp. 109–143, Dec. 2019, doi: 10.1016/j.jechem.2019.01.024.
[6] K. O. Olatunji, N. A. Ahmed, and O. Ogunkunle, "Optimization of biogas yield from lignocellulosic materials with different pretreatment methods: a review," Biotechnol. Biofuels, vol. 14, no. 1, p. 159, Jul. 2021, doi: 10.1186/s13068-021-02012-x.
[7] W. Jerzak, E. Acha, B. Li, W. Jerzak, E. Acha, and B. Li, "Comprehensive Review of Biomass Pyrolysis: Conventional and Advanced Technologies, Reactor Designs, Product Compositions and Yields, and Techno-Economic Analysis," Energies, vol. 17, no. 20, Oct. 2024, doi: 10.3390/en17205082.
[8] W. Jerzak and M. Kuźnia, "Examination of inorganic gaseous species and condensed phases during coconut husk combustion based on thermodynamic equilibrium predictions," Renew. Energy, vol. 167, pp. 497–507, Apr. 2021, doi: 10.1016/j.renene.2020.11.105.
[9] K. J. Abioye et al., "A review of biomass ash related problems: Mechanism, solution, and outlook," J. Energy Inst., vol. 112, p. 101490, Feb. 2024, doi: 10.1016/j.joei.2023.101490.
[10] M. Variny et al., "Advances in Biomass Co-Combustion with Fossil Fuels in the European Context: A Review," Processes, vol. 9, no. 1, Jan. 2021, doi: 10.3390/pr9010100.
[11] J. Nagarajan and L. Prakash, "Preparation and characterization of biomass briquettes using sugarcane bagasse, corncob and rice husk," Mater. Today Proc., vol. 47, pp. 4194–4198, Jan. 2021, doi: 10.1016/j.matpr.2021.04.457.
[12] Y. A. Begum, S. Kumari, S. K. Jain, and M. C. Garg, "A review on waste biomass-to-energy: integrated thermochemical and biochemical conversion for resource recovery," Environ. Sci. Adv., vol. 3, no. 9, pp. 1197–1216, Aug. 2024, doi: 10.1039/D4VA00109E.
[13] Y. Wang et al., "Volatile-char interactions during biomass pyrolysis: Effect of biomass acid-washing pretreatment," Fuel, vol. 340, p. 127496, May 2023, doi: 10.1016/j.fuel.2023.127496.
[14] J. O. Ighalo et al., "Flash pyrolysis of biomass: a review of recent advances," Clean Technol. Environ. Policy, vol. 24, no. 8, pp. 2349–2363, Oct. 2022, doi: 10.1007/s10098-022-02339-5.
[15] N. Ungureanu, N.-V. Vladut, S.-S. Biris, N. Gheorghiță, and I. Mariana, "Biomass Pyrolysis Pathways for Renewable Energy and Sustainable Resource Recovery: A Critical Review of Processes, Parameters, and Product Valorization," Sustainability, vol. 17, p. 7806, Aug. 2025, doi: 10.3390/su17177806.
[16] S. R. Naqvi et al., "Potential of biomass for bioenergy in Pakistan based on present case and future perspectives," Renew. Sustain. Energy Rev., vol. 81, pp. 1247–1258, Jan. 2018, doi: 10.1016/j.rser.2017.08.012.
[17] M. Wieruszewski, K. Mydlarz, M. Wieruszewski, and K. Mydlarz, "The Potential of the Bioenergy Market in the European Union—An Overview of Energy Biomass Resources," Energies, vol. 15, no. 24, Dec. 2022, doi: 10.3390/en15249601.
[18] G. Kataya et al., "Biomass Waste Conversion Technologies and Its Application for Sustainable Environmental Development—A Review," Agronomy, vol. 13, no. 11, Nov. 2023, doi: 10.3390/agronomy13112833.
[19] X. Zou, P. Debiagi, M. A. Amjed, M. Zhai, and T. Faravelli, "Impact of high-temperature biomass pyrolysis on biochar formation and composition," J. Anal. Appl. Pyrolysis, vol. 179, p. 106463, May 2024, doi: 10.1016/j.jaap.2024.106463.
[20] M. Xia et al., "Revealing the anion-dependent effects on potassium-assisted biomass pyrolysis," Fuel, vol. 369, p. 131681, Aug. 2024, doi: 10.1016/j.fuel.2024.131681.
[21] C. Duan et al., "A review on nitrogen transformation mechanism during biomass pyrolysis," J. Anal. Appl.

Pyrolysis, vol. 184, p. 106863, Nov. 2024, doi: 10.1016/j.jaap.2024.106863.
[22] J. Li, K. Xu, X. Yao, and J. Liu, "Investigation of biomass slow pyrolysis mechanisms based on the generation trends in pyrolysis products," Process Saf. Environ. Prot., vol. 183, pp. 327–338, Mar. 2024, doi: 10.1016/j.psep.2024.01.027.
[23] Y. Song et al., "Machine learning prediction of biochar physicochemical properties based on biomass characteristics and pyrolysis conditions," J. Anal. Appl. Pyrolysis, vol. 181, p. 106596, Aug. 2024, doi: 10.1016/j.jaap.2024.106596.
[24] M. Ali, F. Mahmood, C. F. Magoua Mbeugang, J. Tang, X. Xie, and B. Li, "Molten chloride salt pyrolysis of biomass: Effects of temperature and mass ratio of molten salt to biomass," Energy, vol. 316, p. 134634, Feb. 2025, doi: 10.1016/j.energy.2025.134634.
[25] R. Chen, J. Cai, X. Li, and X. Qi, "Discovery and intensity characterization of TDP and PRP based on temperature evolution history during the pyrolysis for large biomass particle," Carbon Resour. Convers., vol. 7, no. 3, p. 100223, Sep. 2024, doi: 10.1016/j.crcon.2024.100223.
[26] G. Li et al., "Regulating phenol tar in pyrolysis of lignocellulosic biomass: Product characteristics and conversion mechanisms," Bioresour. Technol., vol. 409, p. 131259, Oct. 2024, doi: 10.1016/j.biortech.2024.131259.
[27] Z. Liu, J. Zeng, Z. Dong, Y. Chen, H. Yang, and H. Chen, "Insight into the mechanism of lignin amination pretreatment on lignin structure and its pyrolysis property for lignin valorization," Chem. Eng. J., vol. 499, p. 156386, Nov. 2024, doi: 10.1016/j.cej.2024.156386.
[28] J. Zhu and C. Du, "Interaction between lignin and cellulose during the pyrolysis process," Int. J. Biol. Macromol., vol. 265, p. 131093, Apr. 2024, doi: 10.1016/j.ijbiomac.2024.131093.
[29] X. Du and S. Wu, "Effect of lignin modification on the selectivity of pyrolysis products from softwood kraft lignin," J. Anal. Appl. Pyrolysis, vol. 179, p. 106517, May 2024, doi: 10.1016/j.jaap.2024.106517.
[30] M. Yang et al., "Utilization of 2H and 18O isotope labeling of pyrolysis products during lignin pyrolysis," Fuel, vol. 368, p. 131608, Jul. 2024, doi: 10.1016/j.fuel.2024.131608.
[31] S. Wang, G. Dai, H. Yang, and Z. Luo, "Lignocellulosic biomass pyrolysis mechanism: A state-of-the-art review," Prog. Energy Combust. Sci., vol. 62, pp. 33–86, Sep. 2017, doi: 10.1016/j.pecs.2017.05.004.
[32] Y. Ding, O. A. Ezekoye, S. Lu, C. Wang, and R. Zhou, "Comparative pyrolysis behaviors and reaction mechanisms of hardwood and softwood," Energy Convers. Manag., vol. 132, pp. 102–109, Jan. 2017, doi: 10.1016/j.enconman.2016.11.016.
[33] G. Wang et al., "A Review of Recent Advances in Biomass Pyrolysis," Energy Fuels, vol. 34, no. 12, pp. 15557–15578, Dec. 2020, doi: 10.1021/acs.energyfuels.0c03107.
[34] S. Wang et al., "Influence of torrefaction on the characteristics and pyrolysis behavior of cellulose," Energy, vol. 120, pp. 864–871, Feb. 2017, doi: 10.1016/j.energy.2016.11.135.
[35] E. Leng et al., "In situ structural changes of crystalline and amorphous cellulose during slow pyrolysis at low temperatures," Fuel, vol. 216, pp. 313–321, Mar. 2018, doi: 10.1016/j.fuel.2017.11.083.
[36] B. Hu et al., "Formation mechanism of hydroxyacetone in glucose pyrolysis: A combined experimental and theoretical study," Proc. Combust. Inst., vol. 37, no. 3, pp. 2741–2748, Jan. 2019, doi: 10.1016/j.proci.2018.05.146.
[37] Q. Lu et al., "Mechanism of cellulose fast pyrolysis: The role of characteristic chain ends and dehydrated units," Combust. Flame, vol. 198, pp. 267–277, Dec. 2018, doi: 10.1016/j.combustflame.2018.09.025.
[38] G. Dai, G. Wang, K. Wang, Z. Zhou, and S. Wang, "Mechanism study of hemicellulose pyrolysis by combining in-situ DRIFT, TGA-PIMS and theoretical calculation," Proc. Combust. Inst., vol. 38, no. 3, pp. 4241–4249, Jan. 2021, doi: 10.1016/j.proci.2020.06.196.
[39] G. Dai, K. Wang, G. Wang, and S. Wang, "Initial pyrolysis mechanism of cellulose revealed by in-situ DRIFT analysis and theoretical calculation," Combust. Flame, vol. 208, pp. 273–280, Oct. 2019, doi: 10.1016/j.combustflame.2019.07.009.
[40] M. Zheng, Z. Wang, X. Li, X. Qiao, W. Song, and L. Guo, "Initial reaction mechanisms of cellulose pyrolysis revealed by ReaxFF molecular dynamics," Fuel, vol. 177, pp. 130–141, Aug. 2016, doi: 10.1016/j.fuel.2016.03.008.
[41] B. Hu et al., "Mechanism insight into the fast pyrolysis of xylose, xylobiose and xylan by combined theoretical and experimental approaches," Combust. Flame, vol. 206, pp. 177–188, Aug. 2019, doi: 10.1016/j.combustflame.2019.04.052.
[42] X. Zhou, W. Li, R. Mabon, and L. J. Broadbelt, "A mechanistic model of fast pyrolysis of hemicellulose," Energy Environ. Sci., vol. 11, no. 5, pp. 1240–1260, May 2018, doi: 10.1039/C7EE03208K.
[43] J. Li et al., "Comprehensive mechanism of initial stage for lignin pyrolysis," Combust. Flame, vol. 215, pp. 1–9, May 2020, doi: 10.1016/j.combustflame.2020.01.016.
[44] T. Zhang et al., "Initial Mechanisms for an Overall Behavior of Lignin Pyrolysis through Large-Scale ReaxFF Molecular Dynamics Simulations," Energy Fuels, vol. 30, no. 4, pp. 3140–3150, Apr. 2016, doi: 10.1021/acs.energyfuels.6b00247.
[45] D. Carpenter, T. L. Westover, S. Czernik, and W. Jablonski, "Biomass feedstocks for renewable fuel production: a review of the impacts of feedstock and pretreatment on the yield and product distribution of fast pyrolysis bio-oils and vapors," Green Chem., vol. 16, no. 2, pp. 384–406, Jan. 2014, doi: 10.1039/C3GC41631C.
[46] S. V. Vassilev, D. Baxter, L. K. Andersen, and C. G. Vassileva, "An overview of the composition and application of biomass ash. Part 1. Phase–mineral and chemical composition and classification," Fuel, vol.

105, pp. 40–76, Mar. 2013, doi: 10.1016/j.fuel.2012.09.041.
[47] "Protein feeds coproduction in biomass conversion to fuels and chemicals - Dale - 2009 - Biofuels, Bioproducts and Biorefining - Wiley Online Library." Accessed: Dec. 02, 2025. [Online]. Available: https://scijournals.onlinelibrary.wiley.com/doi/abs/10.1002/bbb.132
[48] A. Chavando et al., "Simulation of a Continuous Pyrolysis Reactor for a Heat Self-Sufficient Process and Liquid Fuel Production," Energies, vol. 17, no. 14, Jul. 2024, doi: 10.3390/en17143526.
[49] A. Al-Rumaihi, M. Shahbaz, G. Mckay, H. Mackey, and T. Al-Ansari, "A review of pyrolysis technologies and feedstock: A blending approach for plastic and biomass towards optimum biochar yield," Renew. Sustain. Energy Rev., vol. 167, p. 112715, Oct. 2022, doi: 10.1016/j.rser.2022.112715.
[50] "A review of thermochemical upgrading of pyrolysis bio-oil: Techno-economic analysis, life cycle assessment, and technology readiness - Sorunmu - 2020 - GCB Bioenergy - Wiley Online Library." Accessed: Dec. 03, 2025. [Online]. Available: https://onlinelibrary.wiley.com/doi/10.1111/gcbb.12658
[51] R. F. Beims, C. L. Simonato, and V. R. Wiggers, "Technology readiness level assessment of pyrolysis of trygliceride biomass to fuels and chemicals," Renew. Sustain. Energy Rev., vol. 112, pp. 521–529, Sep. 2019, doi: 10.1016/j.rser.2019.06.017.
[52] A. Al-Rumaihi, M. Shahbaz, G. Mckay, H. Mackey, and T. Al-Ansari, "A review of pyrolysis technologies and feedstock: A blending approach for plastic and biomass towards optimum biochar yield," Renew. Sustain. Energy Rev., vol. 167, p. 112715, Oct. 2022, doi: 10.1016/j.rser.2022.112715.
[53] M.-S. Safdari, E. Amini, D. R. Weise, and T. H. Fletcher, "Heating rate and temperature effects on pyrolysis products from live wildland fuels," Fuel, vol. 242, pp. 295–304, Apr. 2019, doi: 10.1016/j.fuel.2019.01.040.
[54] W. Jerzak, E. Acha, B. Li, W. Jerzak, E. Acha, and B. Li, "Comprehensive Review of Biomass Pyrolysis: Conventional and Advanced Technologies, Reactor Designs, Product Compositions and Yields, and Techno-Economic Analysis," Energies, vol. 17, no. 20, Oct. 2024, doi: 10.3390/en17205082.
[55] W. A. Rasaq et al., "Opportunities and Challenges of High-Pressure Fast Pyrolysis of Biomass: A Review," Energies, vol. 14, no. 17, Aug. 2021, doi: 10.3390/en14175426.
[56] B. Wang, F. Xu, P. Zong, J. Zhang, Y. Tian, and Y. Qiao, "Effects of heating rate on fast pyrolysis behavior and product distribution of Jerusalem artichoke stalk by using TG-FTIR and Py-GC/MS," Renew. Energy, vol. 132, pp. 486–496, Mar. 2019, doi: 10.1016/j.renene.2018.08.021.
[57] H. Xu et al., "Preparation of Co-Mo/γ-Al2O3 catalyst and the catalytic hydrogenation effects on coal-related model compounds," J. Energy Inst., vol. 96, pp. 52–60, Jun. 2021, doi: 10.1016/j.joei.2021.02.005.
[58] Nishu et al., "A review on the catalytic pyrolysis of biomass for the bio-oil production with ZSM-5: Focus on structure," Fuel Process. Technol., vol. 199, p. 106301, Mar. 2020, doi: 10.1016/j.fuproc.2019.106301.
[59] E. M. El-Fawal et al., "Correction: Biofuel production from waste residuals: comprehensive insights into biomass conversion technologies and engineered biochar applications," RSC Adv., vol. 15, no. 21, pp. 16468–16468, May 2025, doi: 10.1039/D5RA90054A.
[60] M. Landrat, M. Abawalo, K. Pikoń, P. A. Fufa, and S. Seyid, "Assessing the Potential of Teff Husk for Biochar Production through Slow Pyrolysis: Effect of Pyrolysis Temperature on Biochar Yield," Energies, vol. 17, no. 9, p. 1988, Jan. 2024, doi: 10.3390/en17091988.
[61] H. Nam, S. C. Capareda, N. Ashwath, and J. Kongkasawan, "Experimental investigation of pyrolysis of rice straw using bench-scale auger, batch and fluidized bed reactors," Energy, vol. 93, pp. 2384–2394, Dec. 2015, doi: 10.1016/j.energy.2015.10.028.
[62] J. L. Santos, M. A. Centeno, and J. A. Odriozola, "Biochar production from cellulose under reductant atmosphere: influence of the total pyrolysis time," RSC Adv., vol. 13, no. 30, pp. 21071–21079, 2023, doi: 10.1039/D3RA03093H.
[63] T. Jalalabadi, M. Glenn, P. Tremain, B. Moghtaderi, S. Donne, and J. Allen, "Modification of Biochar Formation during Slow Pyrolysis in the Presence of Alkali Metal Carbonate Additives," Energy Fuels, vol. 33, no. 11, pp. 11235–11245, Nov. 2019, doi: 10.1021/acs.energyfuels.9b02865.
[64] M. Jouiad, N. Al-Nofeli, N. Khalifa, F. Benyettou, and L. F. Yousef, "Characteristics of slow pyrolysis biochars produced from rhodes grass and fronds of edible date palm," J. Anal. Appl. Pyrolysis, vol. 111, pp. 183–190, Jan. 2015, doi: 10.1016/j.jaap.2014.10.024.
[65] S. D. Ferreira, J. Junges, G. R. Bassanesi, I. P. Lazzarotto, E. Osório, and M. Godinho, "Investigation of the Structure of the Biochar Obtained by Slow Pyrolysis of Elephant Grass during Its Steam Gasification," Chem. Eng. Technol., vol. 42, no. 12, pp. 2546–2555, 2019, doi: 10.1002/ceat.201800680.
[66] A. Trada, A. Chaudhary, D. Patel, and D. S. Upadhyay, "An alternative fuel production from sawdust through batch-type pyrolysis reactor: Fuel properties and thermodynamic analysis," Process Saf. Environ. Prot., vol. 167, pp. 332–342, Nov. 2022, doi: 10.1016/j.psep.2022.09.023.
[67] K. K. B. Suresh Babu, M. Nataraj, M. Tayappa, Y. Vyas, R. K. Mishra, and B. Acharya, "Production of biochar from waste biomass using slow pyrolysis: Studies of the effect of pyrolysis temperature and holding time on biochar yield and properties," Mater. Sci. Energy Technol., vol. 7, pp. 318–334, Jan. 2024, doi: 10.1016/j.mset.2024.05.002.
[68] A. Safavi, C. Richter, and R. Unnthorsson, "Mathematical Modeling and Experiments on Pyrolysis of Walnut Shells Using a Fixed-Bed

Reactor," ChemEngineering, vol. 6, no. 6, p. 93, Dec. 2022, doi: 10.3390/chemengineering6060093.
[69] B. M. Caballero, A. López-Urionabarrenechea, B. Pérez, J. Solar, E. Acha, and I. de Marco, "Potentiality of 'orujillo' (olive oil solid waste) to produce hydrogen by means of pyrolysis," Int. J. Hydrog. Energy, vol. 45, no. 40, pp. 20549–20557, Aug. 2020, doi: 10.1016/j.ijhydene.2020.02.220.
[70] A. Ahmed, M. S. Abu Bakar, A. K. Azad, R. S. Sukri, and N. Phusunti, "Intermediate pyrolysis of Acacia cincinnata and Acacia holosericea species for bio-oil and biochar production," Energy Convers. Manag., vol. 176, pp. 393–408, Nov. 2018, doi: 10.1016/j.enconman.2018.09.041.
[71] M. D. Ibrahim, Y. A. Abakr, S. Gan, L. Y. Lee, and S. Thangalazhy-Gopakumar, "Intermediate Pyrolysis of Bambara Groundnut Shell (BGS) in Various Inert Gases (N2, CO2, and N2/CO2)," Energies, vol. 15, no. 22, p. 8421, Jan. 2022, doi: 10.3390/en15228421.
[72] "Intermediate pyrolysis of Ficus nitida wood in a fixed-bed reactor: effect of pyrolysis parameters on bio-oil and bio-char yields and properties." Accessed: Oct. 12, 2025. [Online]. Available: https://comptes-rendus.academie-sciences.fr/chimie/articles/en/10.5802/crchim.253/
[73] W. Jerzak, N. Gao, I. Kalemba-Rec, and A. Magdziarz, "Catalytic intermediate pyrolysis of post-extraction rapeseed meal by reusing ZSM-5 and Zeolite Y catalysts," Catal. Today, vol. 404, pp. 63–77, Nov. 2022, doi: 10.1016/j.cattod.2021.10.023.
[74] A. Funke, M. Tomasi Morgano, N. Dahmen, and H. Leibold, "Experimental comparison of two bench scale units for fast and intermediate pyrolysis," J. Anal. Appl. Pyrolysis, vol. 124, pp. 504–514, Mar. 2017, doi: 10.1016/j.jaap.2016.12.033.
[75] I. D. V. Torri et al., "Bio-oil production of softwood and hardwood forest industry residues through fast and intermediate pyrolysis and its chromatographic characterization," Bioresour. Technol., vol. 200, pp. 680–690, Jan. 2016, doi: 10.1016/j.biortech.2015.10.086.
[76] C. Boscagli, M. Tomasi Morgano, K. Raffelt, H. Leibold, and J.-D. Grunwaldt, "Influence of feedstock, catalyst, pyrolysis and hydrotreatment temperature on the composition of upgraded oils from intermediate pyrolysis," Biomass Bioenergy, vol. 116, pp. 236–248, Sep. 2018, doi: 10.1016/j.biombioe.2018.06.022.
[77] J. L. Klinger et al., "Effect of biomass type, heating rate, and sample size on microwave-enhanced fast pyrolysis product yields and qualities," Appl. Energy, vol. 228, pp. 535–545, Oct. 2018, doi: 10.1016/j.apenergy.2018.06.107.
[78] K. Rueangsan et al., "Bio-oil production via fast pyrolysis of cassava residues combined with ethanol and volcanic rock in a free-fall reactor," Cogent Eng., vol. 10, no. 1, p. 2156054, Dec. 2023, doi: 10.1080/23311916.2022.2156054.
[79] S. Zinchik et al., "Evaluation of fast pyrolysis feedstock conversion with a mixing paddle reactor," Fuel Process. Technol., vol. 171, pp. 124–132, Mar. 2018, doi: 10.1016/j.fuproc.2017.11.012.
[80] "Fast Pyrolysis of Tropical Biomass Species and Influence of Water Pretreatment on Product Distributions | PLOS One." Accessed: Oct. 12, 2025. [Online]. Available: https://journals.plos.org/plosone/article?id=10.1371/journal.pone.0151368
[81] A. Trubetskaya, P. A. Jensen, A. D. Jensen, M. Steibel, H. Spliethoff, and P. Glarborg, "Influence of fast pyrolysis conditions on yield and structural transformation of biomass chars," Fuel Process. Technol., vol. 140, pp. 205–214, Dec. 2015, doi: 10.1016/j.fuproc.2015.08.034.
[82] B. Urban, Y. Shirazi, B. Maddi, S. Viamajala, and S. Varanasi, "Flash Pyrolysis of Oleaginous Biomass in a Fluidized-Bed Reactor," Energy Fuels, vol. 31, no. 8, pp. 8326–8334, Aug. 2017, doi: 10.1021/acs.energyfuels.7b01306.
[83] P. S. Marathe, R. J. M. Westerhof, and S. R. A. Kersten, "Effect of Pressure and Hot Vapor Residence Time on the Fast Pyrolysis of Biomass: Experiments and Modeling," Energy Fuels, vol. 34, no. 2, pp. 1773–1780, Feb. 2020, doi: 10.1021/acs.energyfuels.9b03193.
[84] M. C. P. dos S. Almeida et al., "Valorization of Wood Residues from Vegetation Suppression during Wind Energy Plant Implementation and Its Potential for Renewable Phenolic Compounds through Flash Pyrolysis: A Case Study in Northeast Brazil's Semi-Arid Region," Forests, vol. 15, no. 4, p. 621, Apr. 2024, doi: 10.3390/f15040621.
[85] R. Kaur, A. Kumar, B. Biswas, B. B. Krishna, and T. Bhaskar, "Investigations into pyrolytic behaviour of spent citronella waste: Slow and flash pyrolysis study," Bioresour. Technol., vol. 366, p. 128202, Dec. 2022, doi: 10.1016/j.biortech.2022.128202.
[86] E. Leng et al., "In situ structural changes of crystalline and amorphous cellulose during slow pyrolysis at low temperatures," Fuel, vol. 216, pp. 313–321, Mar. 2018, doi: 10.1016/j.fuel.2017.11.083.
[87] G. Lopez et al., "Kinetic modeling and experimental validation of biomass fast pyrolysis in a conical spouted bed reactor," Chem. Eng. J., vol. 373, pp. 677–686, Oct. 2019, doi: 10.1016/j.cej.2019.05.072.
[88] J. Y. Park, J.-K. Kim, C.-H. Oh, J.-W. Park, and E. E. Kwon, "Production of bio-oil from fast pyrolysis of biomass using a pilot-scale circulating fluidized bed reactor and its characterization," J. Environ. Manage., vol. 234, pp. 138–144, Mar. 2019, doi: 10.1016/j.jenvman.2018.12.104.
[89] A. Tahmasebi, K. Maliutina, T. Matamba, J.-H. Kim, C.-H. Jeon, and J. Yu, "Pressurized entrained-flow pyrolysis of lignite for enhanced production of hydrogen-rich gas and chemical raw materials," J. Anal. Appl. Pyrolysis, vol. 145, p. 104741, Jan. 2020, doi: 10.1016/j.jaap.2019.104741.
[90] J. Clissold, S. Jalalifar, F. Salehi, R. Abbassi, and M. Ghodrat, "Fluidisation characteristics and inter-phase heat transfer on product yields in bubbling fluidised bed reactor," Fuel, vol. 273, p. 117791, Aug. 2020, doi: 10.1016/j.fuel.2020.117791.

[91] "Optimization of Biomass Pyrolysis Vapor Upgrading Using a Laminar Entrained-Flow Reactor System | Energy & Fuels." Accessed: Oct. 12, 2025. [Online]. Available: https://pubs.acs.org/doi/abs/10.1021/acs.energyfuels.0c00649

[92] A. Bieniek, M. Sieradzka, W. Jerzak, and A. Magdziarz, "Fast pyrolysis of agricultural biomass in drop tube reactor for bio-oil production: Numerical calculations," J. Anal. Appl. Pyrolysis, vol. 176, p. 106241, Nov. 2023, doi: 10.1016/j.jaap.2023.106241.

[93] "Interactions during CO2 Co-gasification of Biomass and Coal Chars Obtained from Fast Pyrolysis in a Drop Tube Furnace | Energy & Fuels." Accessed: Oct. 13, 2025. [Online]. Available: https://pubs.acs.org/doi/abs/10.1021/acs.energyfuels.0c03367

[94] C. E. Efika, J. A. Onwudili, and P. T. Williams, "Influence of heating rates on the products of high-temperature pyrolysis of waste wood pellets and biomass model compounds," Waste Manag., vol. 76, pp. 497–506, Jun. 2018, doi: 10.1016/j.wasman.2018.03.021.

[95] W. Jerzak, M. Wądrzyk, M. Sieradzka, and A. Magdziarz, "Valorisation of tyre waste from a vulcanisation plant by catalytic pyrolysis – Experimental investigations using pyrolysis–gas chromatography–mass spectrometry and drop-tube–fixed-bed reactor," Energy Convers. Manag., vol. 313, p. 118642, Aug. 2024, doi: 10.1016/j.enconman.2024.118642.

[96] A. K. Varma and P. Mondal, "Pyrolysis of sugarcane bagasse in semi batch reactor: Effects of process parameters on product yields and characterization of products," Ind. Crops Prod., vol. 95, pp. 704–717, Jan. 2017, doi: 10.1016/j.indcrop.2016.11.039.

[97] A. Mlonka-Mędrala, P. Evangelopoulos, M. Sieradzka, M. Zajemska, and A. Magdziarz, "Pyrolysis of agricultural waste biomass towards production of gas fuel and high-quality char: Experimental and numerical investigations," Fuel, vol. 296, p. 120611, Jul. 2021, doi: 10.1016/j.fuel.2021.120611.

[98] X. Guo et al., "Catalytic fast pyrolysis of Arundo donax in a two-stage fixed bed reactor over metal-modified HZSM-5 catalysts," Biomass Bioenergy, vol. 156, p. 106316, Jan. 2022, doi: 10.1016/j.biombioe.2021.106316.

[99] J. Solar, B. M. Caballero, A. López-Urionabarrenechea, E. Acha, and P. L. Arias, "Pyrolysis of Forestry Waste in a Screw Reactor with Four Sequential Heating Zones: Influence of Isothermal and Nonisothermal Profiles," Ind. Eng. Chem. Res., vol. 60, no. 51, pp. 18627–18639, Dec. 2021, doi: 10.1021/acs.iecr.1c01932.

[100] F. Campuzano, R. C. Brown, and J. D. Martínez, "Auger reactors for pyrolysis of biomass and wastes," Renew. Sustain. Energy Rev., vol. 102, pp. 372–409, Mar. 2019, doi: 10.1016/j.rser.2018.12.014.

[101] T. A. Memon, X. Ku, V. Vasudev, and S. Ram, "Experimental investigation of co-pyrolysis of fruit peel waste: Impact of blending on thermal degradation behavior, kinetics, and products," Biomass Convers. Biorefinery, vol. 15, no. 12, pp. 18783–18797, Jun. 2025, doi: 10.1007/s13399-025-06550-4.

[102] T. P. S. Livingston, P. Madhu, C. S. Dhanalakshmi, and V. Ayyakkannu, "Non-catalytic and catalytic co-pyrolysis of neem seed cake and plastic waste: an experimental investigation on product distribution, synergistic interaction and characterization," An. Acad. Bras. Ciênc., vol. 97, p. e20241284, 2025, doi: https://doi.org/10.1590/0001-3765202520241284.

[103] S. G. M. Mafo et al., "Unravelling the efficiency removal of 2,4-dinitrophenol on coconut shell biomass-derived activated carbons theoretical and experimental investigation," Biomass Convers. Biorefinery, vol. 15, no. 6, pp. 8821–8841, Mar. 2025, doi: 10.1007/s13399-024-05663-6.

[104] V. Vasudev et al., "An Exploration of Strategies for Conducting Kinetic Analysis of Lignocellulosic and Algal Biomass Pyrolysis," BioEnergy Res., vol. 18, no. 1, p. 64, Jul. 2025, doi: 10.1007/s12155-025-10861-9.

[105] A. P. D. Takahasi et al., "Optimization of liquid fuel production from co-pyrolysis of oil palm fronds and expanded polystyrene using response surface methodology," Case Stud. Chem. Environ. Eng., vol. 11, p. 101074, Jun. 2025, doi: 10.1016/j.cscee.2024.101074.

[106] W. Zhang et al., "An experimental study of the transformation of phosphorus additives during biomass pyrolysis," Fuel, vol. 398, p. 135554, Oct. 2025, doi: 10.1016/j.fuel.2025.135554.

[107] S. Mariyam, M. Alherbawi, G. McKay, and T. Al-Ansari, "A predictive model for biomass waste pyrolysis yield: Exploring the correlation of proximate analysis and product composition," Energy Convers. Manag. X, vol. 25, p. 100831, Jan. 2025, doi: 10.1016/j.ecmx.2024.100831.

[108] K. T. Klasson, "Biochar characterization and a method for estimating biochar quality from proximate analysis results," Biomass Bioenergy, vol. 96, pp. 50–58, Jan. 2017, doi: 10.1016/j.biombioe.2016.10.011.

[109] K. K. Kumar, N. M. Omal, V. K. Sharma, S. B. Kandy, and Ü. Ağbulut, "CO2 storage behavior of rice husk biochar–bitumen mixture at different pressures and temperatures: a detailed experimental investigation," J. Therm. Anal. Calorim., vol. 150, no. 6, pp. 4599–4616, Mar. 2025, doi: 10.1007/s10973-025-14024-y.

[110] N. Rambhatla, T. F. Panicker, R. K. Mishra, S. K. Manjeshwar, and A. Sharma, "Biomass pyrolysis for biochar production: Study of kinetics parameters and effect of temperature on biochar yield and its physicochemical properties," Results Eng., vol. 25, p. 103679, Mar. 2025, doi: 10.1016/j.rineng.2024.103679.

[111] G. Ahmed, P. K. R. Annapureddy, and N. Kishore, "Elucidation of kinetics and thermodynamic properties of Erythrina indica biomass pyrolysis," J. Therm. Anal. Calorim., vol. 150, no. 8, pp. 6127–6143, Apr. 2025, doi: 10.1007/s10973-025-14151-6.

[112] M. Hussain et al., "Co-Pyrolysis of Bamboo and Rice Straw Biomass with Polyethylene Plastic:

Characterization, Kinetic Evaluation, and Synergistic Interaction Analysis," Polymers, vol. 17, no. 15, p. 2063, Jan. 2025, doi: 10.3390/polym17152063.

[113] D. Chen, Y. Li, K. Cen, M. Luo, H. Li, and B. Lu, "Pyrolysis polygeneration of poplar wood: Effect of heating rate and pyrolysis temperature," Bioresour. Technol., vol. 218, pp. 780–788, Oct. 2016, doi: 10.1016/j.biortech.2016.07.049.

[114] N.-B. Mihály, S. Tomasek, N. Miskolczi, V. M. Cristea, T. Chován, and A. Egedy, "Multi-objective optimization of biomass-rich MSW pyrolysis using hybrid multiphase lumped compartment-kinetic model," J. Mater. Cycles Waste Manag., vol. 27, no. 4, pp. 2535–2548, Jul. 2025, doi: 10.1007/s10163-025-02255-y.

[115] M. M. Afessa, F. E. Olu, W. S. Geleta, S. S. Legese, and A. V. Ramayya, "Unlocking the potential of biochar derived from coffee husk and khat stem for catalytic tar cracking during biomass pyrolysis: characterization and evaluation," Biomass Convers. Biorefinery, vol. 15, no. 7, pp. 11011–11026, Apr. 2025, doi: 10.1007/s13399-024-05957-9.

[116] J. Cheng, S.-C. Hu, G.-T. Sun, Z.-C. Geng, and M.-Q. Zhu, "The effect of pyrolysis temperature on the characteristics of biochar, pyroligneous acids, and gas prepared from cotton stalk through a polygeneration process," Ind. Crops Prod., vol. 170, p. 113690, Oct. 2021, doi: 10.1016/j.indcrop.2021.113690.

[117] M. Shahbaz et al., "Investigation of biomass components on the slow pyrolysis products yield using Aspen Plus for techno-economic analysis," Biomass Convers. Biorefinery, vol. 12, no. 3, pp. 669–681, Mar. 2022, doi: 10.1007/s13399-020-01040-1.

[118] J. Ferdous et al., "A comparative investigation of biomass co-pyrolysis with polymeric wastes using electromagnetic induction heating," J. Energy Inst., vol. 120, p. 102023, Jun. 2025, doi: 10.1016/j.joei.2025.102023.

[119] Y. Wang, Z. Wang, X. Li, H. Ge, Y. Zhu, and Q. Li, "Experimental investigation on pyrolysis of coking waste salts: Mechanism of organic compounds removal and salt agglomeration," J. Environ. Manage., vol. 388, p. 125974, Jul. 2025, doi: 10.1016/j.jenvman.2025.125974.

[120] H. Sui et al., "Characterization and mechanistic insights into coke formation on biochar-based catalysts under microwave-assisted biomass pyrolysis," Ind. Crops Prod., vol. 226, p. 120645, Apr. 2025, doi: 10.1016/j.indcrop.2025.120645.

[121] L. Wang, D. Lin, D. Liu, X. Xie, S. Zhang, and B. Li, "Oxidative Pyrolysis of Typical Volatile Model Compounds Under Low Oxygen Equivalence Ratios During Oxidative Pyrolysis of Biomass," Energies, vol. 18, no. 11, p. 2996, Jan. 2025, doi: 10.3390/en18112996.

[122] A. Iqbal et al., "Pyrolysis of macroalgae biomass from Nitella hyalina and its thermokinetics," Biomass Convers. Biorefinery, vol. 15, no. 10, pp. 15211–15223, May 2025, doi: 10.1007/s13399-024-06242-5.

[123] S. A. Yahya et al., "Techno-Economic Analysis of Fast Pyrolysis of Date Palm Waste for Adoption in Saudi Arabia," Energies, vol. 14, no. 19, Sep. 2021, doi: 10.3390/en14196048.

[124] A. L. M. T. Pighinelli, M. A. Schaffer, and A. A. Boateng, "Utilization of eucalyptus for electricity production in Brazil via fast pyrolysis: A techno-economic analysis," Renew. Energy, vol. 119, pp. 590–597, Apr. 2018, doi: 10.1016/j.renene.2017.12.036.

[125] W. Teng, Z. Yu, G. Shen, H. Ni, and X. Ma, "Investigation of the characteristics of microwave-assisted co-pyrolysis of biomass and waste plastics based on orthogonal experimental methods: Thermal degradation, kinetics and product distribution," J. Anal. Appl. Pyrolysis, vol. 189, p. 107083, Aug. 2025, doi: 10.1016/j.jaap.2025.107083.

[126] J. Nagarajan and L. Prakash, "Preparation and characterization of biomass briquettes using sugarcane bagasse, corncob and rice husk," Mater. Today Proc., vol. 47, pp. 4194–4198, 2021, doi: 10.1016/j.matpr.2021.04.457.

[127] Y. Wang et al., "Volatile-char interactions during biomass pyrolysis: Effect of biomass acid-washing pretreatment," Fuel, vol. 340, p. 127496, May 2023, doi: 10.1016/j.fuel.2023.127496.

[128] C. Russo, F. Cerciello, O. Senneca, and B. Apicella, "Challenges and progresses in the chemical investigation of high molecular weight species in condensed pyrolysis products of coal and biomass," J. Anal. Appl. Pyrolysis, vol. 177, p. 106280, Jan. 2024, doi: 10.1016/j.jaap.2023.106280.

[129] W. Treedet and R. Suntivarakorn, "Design and operation of a low cost bio-oil fast pyrolysis from sugarcane bagasse on circulating fluidized bed reactor in a pilot plant," Fuel Process. Technol., vol. 179, pp. 17–31, Oct. 2018, doi: 10.1016/j.fuproc.2018.06.006.

[130] M. Landrat et al., "Assessing the Potential of Teff Husk for Biochar Production through Slow Pyrolysis: Effect of Pyrolysis Temperature on Biochar Yield," Energies, vol. 17, no. 9, Apr. 2024, doi: 10.3390/en17091988.

[131] J. L. Santos, M. A. Centeno, and J. A. Odriozola, "Biochar production from cellulose under reductant atmosphere: influence of the total pyrolysis time," RSC Adv., vol. 13, no. 30, pp. 21071–21079, Jul. 2023, doi: 10.1039/D3RA03093H.

[132] T. Jalalabadi, M. Glenn, P. Tremain, B. Moghtaderi, S. Donne, and J. Allen, "Modification of Biochar Formation during Slow Pyrolysis in the Presence of Alkali Metal Carbonate Additives," Energy Fuels, vol. 33, no. 11, pp. 11235–11245, Nov. 2019, doi: 10.1021/acs.energyfuels.9b02865.

[133] "Design and Experimental Evaluation of a Pilot-Scale Screw Pyrolysis Unit with Producer Gas Based Heating | Waste and Biomass Valorization." Accessed: Nov. 23, 2025. [Online]. Available: https://link.springer.com/article/10.1007/s12649-025-03092-8

[134] "An experimental Study on Biomass Pellets of Saw-Dust with Different Binders Based on Gasification and Multi-Criteria Decision Making | Waste and Biomass Valorization." Accessed: Nov. 23, 2025. [Online]. Available:

https://link.springer.com/article/10.1007/s12649-025-02988-9
[135] "Investigating the Predictive Capabilities of MARS for Biomass Pyrolysis Kinetics: A Case Study on an Oil Palm Empty Fruit Bunch | ACS Omega." Accessed: Nov. 23, 2025. [Online]. Available: https://pubs.acs.org/doi/10.1021/acsomega.4c09789?ref=PDF
[136] "'Kinetic modelling of biomass pyrolysis: A new lumped scheme for xylan-based hardwood hemicellulose' - ScienceDirect." Accessed: Nov. 23, 2025. [Online]. Available: https://www.sciencedirect.com/science/article/pii/S2590174525002624?via%3Dihub
[137] C. B. Ugwuodo, "Investigation of process parameters for producing bio-oil from luffa cylindrical fiber in a fixed bed reactor using pyrolysis process," LAUTECH J. Eng. Technol., vol. 19, no. 2, pp. 126–137, Jun. 2025.
[138] "Insight into the catalytic role of industrial solid waste in improving gas quality during biomass pyrolysis - ScienceDirect." Accessed: Nov. 23, 2025. [Online]. Available: https://www.sciencedirect.com/science/article/pii/S2588913325000377?via%3Dihub
[139] L. Kapoor and N. R. Pranav, "Estimating the Effect of Biomass to Catalyst Ratio on the Bio-oil and Char Yield in the Pyrolysis of Spent Coffee Grounds," ES Energy Environ., vol. Volume 27 (March 2025), no. 0, p. 1383, Jan. 2025.
[140] G. Lezcano et al., "Linking microalgae characteristics with their fast pyrolysis products," J. Anal. Appl. Pyrolysis, vol. 191, p. 107170, Oct. 2025, doi: 10.1016/j.jaap.2025.107170.
[141] X. Li, F. Yu, X. Chen, and Y. Nie, "In-situ and ex-situ catalytic pyrolysis of lignin in rotary kilns with metal-modified acidified ZSM-5," Fuel, vol. 401, p. 135946, Dec. 2025, doi: 10.1016/j.fuel.2025.135946.
[142] D. Huang et al., "Investigation on in-situ and ex-situ catalysis of metal salt in biomass photo-thermal pyrolysis: Effects on decoupled primary and secondary reactions," Fuel, vol. 405, p. 136638, Feb. 2026, doi: 10.1016/j.fuel.2025.136638.
[143] S. R. Naqvi, Y. Uemura, and S. B. Yusup, "Catalytic pyrolysis of paddy husk in a drop type pyrolyzer for bio-oil production: The role of temperature and catalyst," J. Anal. Appl. Pyrolysis, vol. 106, pp. 57–62, Mar. 2014, doi: 10.1016/j.jaap.2013.12.009.
[144] P. K. Kanaujia, Y. K. Sharma, U. C. Agrawal, and M. O. Garg, "Analytical approaches to characterizing pyrolysis oil from biomass," TrAC Trends Anal. Chem., vol. 42, pp. 125–136, Jan. 2013, doi: 10.1016/j.trac.2012.09.009.
[145] "Understanding the product distribution from biomass fast pyrolysis - ProQuest." Accessed: Dec. 07, 2025. [Online]. Available: https://www.proquest.com/openview/368d55138c826c7f15ee34e6965e511e/1?pq-origsite=gscholar&cbl=18750
[146] "Thermochemical Processing of Miscanthus through Fluidized-Bed Fast Pyrolysis: A Parametric Study - Wang - 2018 - Chemical Engineering & Technology - Wiley Online Library." Accessed: Dec. 08, 2025. [Online]. Available: https://onlinelibrary.wiley.com/doi/full/10.1002/ceat.201700486

Appendix 1

Overview of the process factors influencing pyrolysis and co-pyrolysis

Pyrolysis Type	Reactor type & Feed Rate	Process Temp. °C (Weight of Sample)	Heating Rate (°C/min)	Residence Time	Particle Size of Biomass	Types & Composition of Biomass	Carrier Gas Type & Flow Rate	Ref.
Intermediate	Vertical tubular reactor (VTR)	110 °C to 900 °C	10°C/min	10 min	1.18 mm	Bambara Groundnut Shell	N_2 20 mL/min	[47]
Intermediate	-	500°C	4 mg sample, 10°C/min	7 min	300–750 µm	Rapeseed meal	Air & N_2 100 mL/min for 5 mins	[48]
Fast Intermediate	Fluidized Bed Reactor STYX Reactor (feed rate 10 kg /h)	500 °C	High	1-2 h	1 mm	Hybrid poplar, Wheat straw and a blend biomass	N_2 and quartz sand (0.4-0.8 mm) fluidization velocity 0.2 m/s	[49]
Intermediate Pyrolysis Fast Pyrolysis	Fixed Bed Bubbling Fluidized Bed (feed rate 700 g/h)	400, 550 and 700 °C (5, 7 and 9g) 500 °C	100 °C/min	10 to 30 s	0.40-92mm	Eucalyptus sp. (hardwood) and *Picea abies* (softwood)	N_2 1 mL/min	[50]
Intermediate Pyrolysis	STYX Pyrolysis Reactor (4kg/h)	350-500 °C (50 mg)	200 K/min	2.5-40 min	-	Chicken Manure	N_2	[51]
Intermediate Pyrolysis	STYX Reactor (Feed rate 2kg/h)	80, 150, 250, 350°C	15 K/min	10 min	100µm >	Beech Wood, Wheat Straw	N_2, H_2 1.6L/min	[52]
Fast Pyrolysis	Microwave-assisted fast pyrolysis (MEFP) reactor	600°C (>1g)	200 °C/s	<0.5 sec (1.05g sample) <0.25sec (for the 4.50g)	2 mm	Agriculture residues, herbaceous energy crops, woody feedstock and blended feedstock	N_2 0.9L/min at STP	[53]
Fast Pyrolysis	Free-fall Reactor (Feed rate 200 g/h)	450 and 550 °C	10 °C/s	~3.6 s	0.2 and 0.5 mm	Cassava residues combined with ethanol and volcanic	N_2 flow rate of 4L/min	[54]
Fast Pyrolysis	Mixing-paddle reactor (Sand feed rate 1500 g/h, biomass feed rate 100g/h)	500 °C (Sample 5-10 kg)	110 °C/s	10 sec	2 mm	Corn stover, hybrid poplar, clean loblolly pine, wood waste, miscanthus	N_2 0.24L/min	[55]
Fast Pyrolysis	Fluidized bed reactor	450°C (7.5 g of feedstock)	~400°C/s	1.5 to 2.5 mins	200µm (biomass)	Bana grass	-	[56]
Fast Pyrolysis	Wire mesh reactor	1700 °C	5000 °C/s, and pressure up to 50 bar	1-4 s	0.05-0.2 mm 0.25-0.355 mm 0.425-0.6 mm 0.6-0.85 mm	Danish wheat straw, Pinewood, leached Danish wheat straw, straw and rice husk	-	[57]
-	-	1250 °C (sample of 5mg)	0 to 1000 C/min	-	-	Jerusalem artichoke stalk	N_2 100ml/min	[58]
Flash Pyrolysis	Fluidized Bed	250-610°C	-	0.2 0.3 s	1-8.4mm	Milled soybean	N_2 Pressure of 20 Psi	[59]
Fast Pyrolysis	Fluidized Bed	515°Cforbagasse and at 485°C for pinewood.	~5000 °C/s	20 msec	Pinewood (0.5-2 mm, <150µm, bagasse (<150µm)	acid-leached bagasse and pinewood, 5×10^{-3} to 100 kPa	-	[60]
Flash Pyrolysis	Analytical Pyrolizer	30 to 900°C (Sample of 10 mg)	10°C/min	20 sec	0.150 mm	Non-uniform-sized sawdust	N_2 50 mL/min	[61]
Slow Pyrolysis & Flash Pyrolysis	-	450 °C	20°C/s	-	0.5-1.5 mm	Spent citronella biomass	-	[62]
Slow Pyrolysis	-	40 to 600°C (sample of 2g)	5 K/min	-	53-96µm	A crystalline cellulose and amorphous cellulose	N_2 100mL/min	[63]
Fast Pyrolysis	Conical spouted bed reactor	450, 500 and 550°C (100g)	-	0.56 and 1.69s	1-2mm	Pinewood sawdust	N_2 2, 6 and 11 L/min	[64]

Fast Pyrolysis	Fluidized bed (42kg/h)	800°C (Sample of 100g)	10°C/min	30 mins	2-3mm.	Sawdust, empty fruit bunch, and giant Miscanthus	Helium 100mL/min	[65]
Lignite pyrolysis	Pressurized entrained-flow reactor (feed rate 0.5 g/min)	600-900 °C and pressure 0.1-4.0 MPa (sample of 30 gm)	1700-5900 K/s	5-6 s	125-300 µm	Hailar lignite	N_2 1.0-6.4 L/min	[66]
Fast Pyrolysis	Bubble-fluidized bed reactor (100g/h)	773K	-	-	0.4 to 1 mm (sand particle) 0.2-0.5 mm (biomass)	Virgin cellulose, virgin hemicellulose, virgin lignin	N_2 Velocity 0.36 m/s	[67]
Catalytic Fast pyrolysis	Vapor-phase upgrading reactors (5-40 g/h of biomass) and 50-475 g/h catalyst)	550°C (sample of (~0.04 g)	3°C/min	4 hrs.	250-125 µm	Yellow pine	N_2	[68]
Fast pyrolysis	Fluidized beds, Auger, and Drop tube reactor (10-30 g/h)	500-700°C	-	-	250-750 µm	Oat and corn Straw	N_2 3-5 L/min	[69]
Fast pyrolysis	Fluidized bed Auger Drop-tube reactor (10-30 g/h)	500-700 °C	-	-	250-750 µm	Oat and corn straw	N_2 3-5 L/min	[70]
Fast pyrolysis	Drop-tube reactor (10±1) g/h)	800, 900, 950, and1000°C	~104°C/s	60min	>10µm	Olive residue and Soma lignite	N_2 4 slpm	[71]
-	Drop-tube-fixed-bed reactor)	25-800°C (sample of 5 mg)	10°C/min	20 s	500-800 µm	Car tire	N_2 40 mL/min	[72]
-	Semi batch reactor	350-650°C	10 & 50°C/min	20 min	0.5-0.6 mm 0.25-0.5 mm 0.6-1 mm	Sugarcane bagasse	N_2 100 cm^3/min	[73]
-	Horizontal fixed bed reactor	800°C	5,90 and 350 °C/min	9 s	~1 mm	Pinewood sawdust	N_2 100 ml/min	[74]
-	Semi-batch vertical reactor	300, 400, 500, and 600 ◦ C (5 mg)	10 K/min	15 min	< 1 mm	Oat straw	N_2 50 ml/min	
Catalytic Fast pyrolysis	Two-stage fixed bed reactor	500°C (40 g)	10°C/min	30 min	0.18-0.42 mm	Arundo donax	N_2 3×10^{-4} m^3/min	[75]
Slow	Auger reactor Tubular reactor	40 and 240 °C	8-150 °C/min	5 and 10 min	-	Pinus radiata	Helium 2.3 mL/min	[76]
Intermediate	Auger reactor (1-3.5 kg/h)	450-500 °C	100 °C/s	< 2 s	28% of 2-3mm, 47% of 1-2mm, 19% of 0.5-1mm, and 6% of 0.1-0.5mm	Fresh balsam fir shavings	-	[77]
Co-pyrolysis	Horizontal tube reactor	150-850 °C (10 mg)	8, 16, 24, and 32 °C/min	-	0.2 mm	Pomelo peel, papaya peel, and watermelon peel	N_2 50 mL/min	[78]
Co-pyrolysis	Stainless-steel reactor	350, 400, 450, 500, and 550°C.	20°C/min	30 minutes	-	Plastic waste and Neem seed cake	-	[79]
Fast pyrolysis	-	600°C (50 mg)	5°C/min	2 hrs.	0.22-mm	Coconut shells	N_2	[80]
Hydro-thermal & fast pyrolysis	-	190°C and 600°C (10 mg)	10°C/min	-	0.212 mm	Lignocellulosic and algal feedstocks	N_2	[81]
Intermediate	Fixed-bed reactor	300-500°C	13.91-14.99°C/min.	2 hrs.	2 mm and 1.4 mm (PS) (EPS)	Expanded polystyrene, oil palm fronds	N_2 20 mL/min	[82]
Fast pyrolysis	Fixed-bed reactor	550°C (2 g)	10°C/min	30 min.	Smaller than 470 µm and 420 µm	Pine wood and wheat straw	N_2 3 L/min	[83]
Intermediate& Fast pyrolysis	CHNSO analyzer	350, 400, 450, 500, 550 & 600°C (30 g)	10°C/min	between 30 and 120 min	2 -5 mm (HDPE)	Olive pomace (OP) and plastic wastes	N_2 1.2 mL/min	[84]
Intermediate and Fast Pyrolysis	Batch Reactor	300-700°C	-	0.5-4 hrs.	-	Cellulose, wood, cow manure, poultry manure, saw dust blend, pine wood chips, wheat straw, grass.	-	[85]

Intermediate	$\frac{1}{4}$-inch seamless stainless-steel	500°C (~ 2 g of activated biochar)	10°C/min	-	1 mm	Rice husk	N_2 3 mL/min	[86]
Fast & Flash pyrolysis	Stainless steel semi-batch reactor	400, 600 & 900°C	10, 30, and 50°C/min	45 min	750 µm	Mixed wood sawdust (MWS)	N_2 100 mL/min	[87]
Fast pyrolysis	-	25-900°C	10, 20, 30, 40 K/min	-	600-micron mesh sieve	*Erythrina indica* (EI)	N_2 20-40 mL/min	[88]
Co-pyrolysis	Micro-scaled thermogravimetric analysis (TGA) equipment	700°C (5 mg)	5, 10, and 20°C/min	5 min	Biomass sample < 450 µm, polythene <50 µm	Rice straw, Bamboo with a plastic polyethylene	High-purity N_2 100 mL/min	[89]
Slow pyrolysis	Fixed-bed reactor (Lab-scale)	600, 550, 500, 450, 400°C (10gm of sample)	10, 30, 50°C/min	10 min	0.25-0.42mm	Poplar wood sawdust	High-purity N_2 200 mL/min	[90]
Fast pyrolysis	Two-stage pyrolysis reactor	500°C	-	40 min	-	Municipal solid waste (utilized catalyst Ni/ZSM-5)	N_2 75 mL/min	[91]
Slow Pyrolysis	Fixed-bed reactor (Batch type)	700, 550, 450, 350°C	-	4 hrs.	< 500 µm	Khat stems & Coffee husk	-	[92]
Slow pyrolysis	Vertical pyrolytic reactor (200g sample)	300, 350, 400, 450, 500, 550°C (200g sample)	2°C/s	2hrs.	1-3cm	Cotton stalk	N_2 20mL/min	[93]
Slow pyrolysis	Gibbs Reactor	450°C	10°C/min	30 min	-	Cellulose, hemicellulose, lignin	-	[94]
Co-pyrolysis	Induction Heated Fixed-Bed Reactor	450°C (500g feedstock)	20°C/min	50 min	0.5-2 mm	Vegetable wastes, tire scraps, water hyacinth and low-density polyethylene	N_2 For 3 min	[95]
Fast Pyrolysis	Tubular Furnace	20°C -650°C	10°C/min	120 min	-	Cooking waste salts	N_2 100 mL/min	[96]
Microwave-Assisted Catalytic Pyrolysis	Microwave Reactor	450°C, 550°C, 650°C (4g of feedstock)	-	60 min, 40 min, 20 min	-	Poplar wood chips (ZSM-5 with a Si/Al)	N_2 200 mL/min for 15 min	[97]
Fast Pyrolysis	Two-Stage Quartz-Tube Reactor system	400 or 500°C (0.5 g of feedstock)	-	15 min	-	Biomass volatile	N_2 250 mL/min oxidation gas of N_2 mixture 50 mL/min	[98]
Flash Pyrolysis	-	25°C-800°C (5mg of feedstock)	5, 10, 20°C/min	-	500µm	Macroalgae *Nitella hyalina*	N_2 60 mL/min 30 min	[99]
Fast Pyrolysis	Fluidized bed reactor	525°C (10 tons/day)	>100°C/min	30-1500 ms	<1mm	Date palm waste	-	[100]
Fast Pyrolysis	Fluidized bed reactor	- 200 tons/day	-	-	2mm	Eucalyptus tress	N_2	[101]
Microwave-Assisted Co-pyrolysis	Microwave Reactor	900°C (3g of sample)	20, 40, 50°C/min	-	-	Eucalyptus wood and polypropylene	N_2 High purity (99.9%) 80mL/min	[102]
Slow Pyrolysis	Batch Charcoal kiln Reactor	- 1kg/batch	-	40 min	1 mm	Corncob, Sugarcane, Rice Husk, Firewood charcoal	Allow some oxygen	[103]
Slow pyrolysis	Fixed-bed Reactor	600°C (30g of sample)	20, °C/min	30min	0.9-2mm	Poplar wood and acid washed poplar wood	N_2 200mL/min	[104]
Fast/very fast	1. Drop-tube reactor 2. Heated Strip reactor	1000-1800°C	60000-600000 °C/min	-	-	Softwood bark, hardwood, pine, poplar, straw, rice husk, coal	N_2 -	[105]
Fast Pyrolysis	Circulating Fluidized bed reactor (18-45kg/h)	Optimum 480°C	-	-	327 µm	Sugarcane bagasse	LPG 5-7 m/s	[106]

Slow Pyrolysis	Fixed Bed Reactor (1kg/run)	400, 450, 500°C (max. biochar yield 400°C	4.2°C/min	120 min	<0.5 mm	Teff husk	N_2 30 mL/min	[107]
Slow/Intermediate Pyrolysis	Auger reactor (~10g/min)	500°C (300 g of batch)	4°C/min	20-25 min	-	Rice straw	N_2 10 L/min	[108]
Slow Pyrolysis	Batch steel tube reactor (50 g/run cellulose)	700°C (50 g)	5, 10, 20°C/min	1, 120, 240 min	5-250 µm	Microcrystalline cellulose	N_2/ H_2 200 mL/min	[109]
Slow Pyrolysis	Thermogravimetric analyzer	600, 750, 900°C	-	-	0.2 mm maintain precise particle size	Sawdust of Eucalyptus Pilularis	N_2/Argon	[110]
Fast Pyrolysis	Screw Reactor (Feed rate 8, 10, 16 kg/h)	400°C and 500°C	-	5, 10, 15 min of sample	<1.5mm	Grinded rice straw	Gas flow 12 Nm^3/h	[111]
Gasification	Fixed-bed reactor	1000°C (10mg of sample)	20°C/min	-	80-100 μm	Waste rice starch water, burnt engine oil & saw dust.	Air 100mL/min	[112]
Fast Pyrolysis	CHNS/O analyzer	800°C	5, 7.5, 10 and 12.5°C/min	-	100 μm	Oil Palm Empty Fruit bunch	N_2 50mL/min	[113]
Flash Pyrolysis	Thermogravimetric analyzer	>950°C (sample of 10-12mg)	3, 10, 20, 50, and 100°C/min	-	-	Beechwood-derived Xylen	He 275mL/min	[114]
Fast Pyrolysis	Stainless steel tube Reactor (Not properly mentioned)	200-700°C	10°C/min	-	1, 3, 4, 5, 6, 7 mm	Luffa cylindrica fiber	N_2 2.5L/min	[115]
Catalytic Pyrolysis	Quartz tube Reactor	600°C	5°C/min	Temp. maintain for 15 mins	<0.178 mm	Peanut shells	N_2 20mL/min	[116]
Catalytic pyrolysis	Fixed-bed reactor	600°C	10°C/min	Sample residence time 10 mins	-	Coffee robusta and arabica (ZnO used as catalyst)	N_2 1.5mL/min	[117]
Fast Pyrolysis	Pyroprobe	450, 550, 650°C	~125-150°C/s	60 s	~50 μm	8 Microalgae species	He 0.8 mL/min	[118]
In-situ & Ex-situ Catalytic Pyrolysis	Rotary Klin	500°C	33.33°C/min	1hr.	-	Dealkaline	High-purity N_2 400mL/min	[119]
In-situ & Ex-situ Catalytic Pyrolysis	Two-Stage Photo-Thermal Reactor	750°C	200°C/min	4 mins	50-100 μm pellets	Rapeseed Cake	N_2 200mL/min	[120]
Catalytic Pyrolysis	Bench-Scale Tubular	500°C	-	-	0.10-0.14mm	Corn Stover	N_2 100mL/min	[121]
Co-pyrolysis with catalytic Reforming	Two-Zone Tube Furnace	500-800°C	-	20 mins	-	Corn Cob & Polyethylene	N_2 No flowrate specified	[122]
Thermogravimetric	-	30-900°C	10, 20, 40°C/min	20 mins	0.10-14mm	Wheat straw & Pine sawdust	High-purity N_2 100mL/min (200mL/min for purge)	[123]
In-situ Catalytic Pyrolysis	Fixed-Bed Reactor	600°C (0.5 g bamboo)	15°C/min	-	-	Bamboo	N_2 90mL/min	[124]
Molten nitrate salt pyrolysis	Batch Reactor	300. 350°C	-	10 mins	2 mm	Cotton stalk, waste paper	N_2 700mL/min	[125]
Thermogravimetric	Thermogravimetric analyzer	50-900°C (5±0.1g)	20, 40 & 50°C/min	-	-	Eucalyptus wood and polypropylene	N_2 80mL/min	[126]
Thermogravimetric	TGA analyzer	800°C	10 K/min	-	1-12 mm	Byproducts from woodcutting	-	[127]
Thermogravimetric	TGA analyzer	30-800°C	10, 20 and 30 K/min	-	0.15 mm	Rubber Seed oil	Argon 50ml/min	[128]
Thermal pyrolysis	-	300-1000°C	5-800°C/min	-	-	Sunflower-oil cake, Walnut shell, Rice Husk, Pine bark	-	[129]
Thermogravimetric	-	30-800°C	10 & 200°C/min	-	4 mm	Pinewood	N_2 100mL/min	[2]
Flash Joule Heating	Graphite boat reactor	800, 900, 1000°C (1 g of alkali lignin)	245-290°C/s ~22-27°C/s	20 s 5 min	-	Alkali Lignin	Argon 50mL/min	[130]

Oxidative pyrolysis	Quartz-tube Fluidized-Bed reactor	600°C (0.5 g biochar)	-	~5.75 s for gas 10 mins for biochar	90-180 µm	Biochar from Pine wood dust	Mixture of air & N_2 300mL/min	[131]
Reductive Pyrolysis	Tube Furnace	400-800°C	10°C/min	30-150 mins	-	Cellulose, Xylan, Lignin	N_2	[132]
Slow pyrolysis	Thermal fixed bed reactor	750°C (15g of hemp Powder)	20°C/min	3hr	0.2 mm	Hemp	N_2 50mL/min	[133]
Catalytic Fast pyrolysis	Micro-pyrolyzer	600°C (0.1±0.01g)	20°C/mS	20 s	-	Cotton-stalk and polypropylene	N_2 1mL/min	[134]
In-situ Catalytic Co-pyrolysis	Tube Furnace with a quartz crucible	850°C	10°C/min	20 min	-	Pistachio Tailings Lignin	N_2 100mL/min	[135]
Fast Pyrolysis	Graphite Tube reactor	800, 900, 1000°C (0.2 g of alkali)	25-300°C/S	12 s	-	Alkali Lignin	-	[136]
Analytical pyrolysis	Custom Quartz reactor	- (10±0.1mg)	-	-	-	Anthracite, Bituminous coal, Lignite	N_2 100mL/min	[137]
Molten salt pyrolysis	Crucible reactor with bubble tube	750°C (~2.3 g)	-	20 mins	<0.25 mm	Algae	N_2 200mL/min	[138]
Thermogravimetric	TGA analyzer	30-900°C	10°C/min	-	< 74 µm	Wheat straw, Rice straw	N_2 100mL/min	[139]
Microwave - assisted Pyrolysis	Multimode Microwave oven with quartz	800°C (20 g of feedstock)	-	-	0.5-1mm	Rice straw, Bagasse, Pine wood	N_2 100mL/min	[140]
Thermogravimetric	TGA analyzer	850°C (20 mg)	20°C/min	-	-	Arginine	N_2 20mL/min	[141]
Slow pyrolysis	Electrically Heated vessel reactor	400°C	5°C/min	11 hrs.	2 mm	Rhodes grass and Fronds of Date Plam	N_2	[142]

Appendix 2

Biomass type, analytical techniques, product phase, and chemical families in pyrolysis

Biomass Type	Pyrolysis Temperature (°C)	Analytical Method	Identified Intermediate Compounds	Product Phase	Chemical Families	Ref.
Eucalyptus woodlot	500°C, 550°C, 600°C, 650°C and 700°C	1. TGA/DSC for thermal decomposition behavior 2. GC/MS for organic compositions and condensable, liquid 3. OED for influence of various factors	1. Furan based compound 2. Olefins 3. Free radicals	1. Liquid (Bio oil) 2. Gas (Syngas) 3. solid (Biochar)	1. Acids, alcohols, ethers, phenols, aldehydes, and ketones (from EW). 2. Alkanes and alkenes $C_8 - C_{15}$ (from PP). 3. Styrene and other monocyclic aromatic hydrocarbons (MAHs). 3. PAHs, or polycyclic aromatic hydrocarbons, such as phenol, fluorene, and naphthalene. 4. Light Hydrocarbon, CO, and CO_2	[125]
Pinewood block	600°C	1. GC/MS 2. FID 3.TCD utilized to determine the impact of biomass particle size, heating rate and shape 4. TG/FTIR used to characterize distributions of products	-	1. Liquid (Bio oil) 2. Gas (Syngas) 3. solid (Biochar)	Liquid product (Bio-oil): 1. Ketones 2. Aldehydes 3. Acid 4. Esters 5. Alcohols, 6. Phenols Gas Products: 1. CO_2 2. CO	[2]
Pine sawdust	600°C	1. GC analyzed for oxidation of biochar 2. FTIR used to determine functional surface group of biochar 3. BET used for determining specific surface area of biochar 4.	Not explicitly specified	1. Gas 2. solid (oxidized biochar)	Gas Products: 1. CO, CO_2 2. H_2 3. light hydrocarbons (CH_4, C_2^+) Solid (biochar) Products: 1. Hydroxyl (-OH), carboxyl (-COO), phenolic (C-OH), aromatic (C=C, C-H), aliphatic (C-H)	[131]
Cellulose, Hemicellulose, Lignin-based biomass	600°C	1. ICP-OES (quantifying metal content) 2. SEM 3. XRD 4. XPS 5. TG/DSC 6. HSC chemistry software for thermodynamic calculations.	1. Ph-O- radicals 2. Carbon centered radicals 3. Benzyl radicals 4. Reactive oxygen species 5. Li_2O	1. Solid 2. Liquid (Leachate) 3. Gas	Gas Products: 1. CO, H_2, CH_4 2. CO_2 3. Volatile Organic Compounds Solid Products: 1. Lithium Salt (Li_2CO_3) 2. Ni, Co 3. MnO 4. Biochar	[132]
Pheonix Tree Leaves	200-400°C	1.TG/DTG 2. Py-GC/MS 3. XRD 4.SEM 5. BET for surface area analysis 6. XRF for elemental compositions of solids	1. Anhydro-sugars generates Aldehydes, ketones, alcohols 2. Unstable non carbonized organic matter 3. Oxygenated compounds (Co oxidation)	1. Solid (Biochar) 2. Liquid (Tar/Bio-oil) 3. Gas (Syngas)	Gas Products: 1. H_2, CO, CH_4 2. CO_2 Liquid Products: 1. Hydrocarbons 2. Phenols, Alcohols, Ketones, Esters, Aldehydes, Acid, Furan, Anhydro-sugars 3. N_2 containing compounds Solid Products: 1. Co, CoO, MnO, CaO 2. Carbonaceous Matrix	[135]
Alkali Lignin	800-1000°C	1. Elemental Analysis 2. XRD 3. FTIR 4. Raman Spectroscopy 5. XPS for analyze surface chemistry and bonding 6. BET surface analysis 7. Zeta potential analysis and particle size 8. Four-point probe conductivity test	1. Condensable volatiles (pore blockage) 2. Alkyl, methoxy, phenolic hydroxyl group	Solid (Biochar)	Solid Products: 1. Aromatic carbon structures/Graphitic carbon 2. C-O, Hydroxyl (-OH), Methoxy (-OCH_3), Carbonyl (C=O), Aliphatic C-H/C-C 3. Metal Oxides from ash	[136]

		9. Bomb calorimeter (HHV)				
Inorganic Nano-choloropsis	750°C	1. GC with TCD/FID 2. XRD 3. XRF 4. Ion meter 5. DSC Fact stage software (Thermodynamic simulation)	1. Active Char 2. Volatiles (Secondary Reaction)	1. Liquid (Bio-oil) 2. Gas 3. Char 4. Salt matrix (reacted/molten salt)	Gas Products: 1. H_2, CH_4 2. C_2-Hydrocarbons 3. CO, CO_2 Solid Products: 1. Alkali salts: NaOH, KCl, NaCl, Na_2CO_3 2. Precipitates: $CaCO_3$, $MgCO_3$, $Mg_2Cl(OH)_3$, $Na_2Mg_3Fe_2Si_8O_{22}(OH)_2$ 3. Na_2SO_4, SiO_2, Na_2SiO_3	[137]
Wheat and rice straw	900°C	1. In-situ Synchrotron DRIFTS (Used to tracking functional group changes) 2. Peak Deconvolution (to quantify in overlapping absorption bands) 3. TG/DTG (provides macroscopic context of mass loss)	1. Free radicals 2. C-O and CH_3 radicals 3. Small molecular components	1. Liquid (Bio-oil) 2. Gas 3. Solid (char)	Gas Products: 1. CH_4, CO, CO_2, H_2O, C_3H_6, C_4H_8, C_3H_8, C_4H_{10} Liquid Products (Bio-Oil): 1. Aliphatic hydrocarbons ($C_6 - C_{10}$), Toluene, xylene 2. Naphthalene, Phenanthrene.	[138]
Rice straw, Bagasse, Pine wood, Prosospis Julifora	500°C	1. Standard Fuel Analysis (Ultimate, Proximate, HHV) 2. GC, GC/MS 3. BET, XRD, SEM/EDS, XRF, FTIR	1. Methyl radicals (• CH_3) 2. H• radicals 3. Anhydro-sugars 4. Pyrolysis vapors	1. Gas (non-condensable) 2. Liquid (bio-oil) 3. Solid (Biochar)	Gas Products: 1. H_2, CO, CH_4, CO_2 Liquid Products: 1. Phenol, P-cresol, Guaiacol, Syringols 2. 1-hydroxy-2-Butanone, Tetra-decanoic, Hexa-decanoic 3. Alkanes ($C_{10} - C_{20}$), 1-nonadecene.	[139]
Arginine	700°C	1. TG/DTG 2. FTIR 3. Py-GC/MS 4. Reactive Force Field Molecular Dynamics 5. Density Functional Theory (DFT)	H•, • CH_3, •NH_2, •CN, •COOH	1. Gas 2. Liquid (Condensable Volatiles) 3. Solid (carbonized residue)	Gas Products: NH_3, HCN, HCNO, CO_2, C_2H_4, CH_4, H_2, H_2O Liquid Products: 1. Olefins (Ethylene) 2. Pyridine, Pyrrole, Piperidi-nones 3. Cyclohexen-1 4. Acids, Phenols, Alcohols	[140]
Dealkaline lignin	500°C	1. Gas Chromatography (GC) 2. Mass Spectroscopy (MS)	1. Phenols, Guaiacols, Aldehydes, Ketones, Ether & Aromatic compounds	1. Liquid (Bio-oil) 2. Non- condensable Gas 3. Solid (Biochar)	Liquid Products: 1. Phenols, 2-Methyl-phenol, 3-Methyl-pheno, 2,6- Dimethyl-phenol 2. Guaiacol, Cresol, 2- Methoxy-3-methyl-phenol 3. Vanillin, Apocynin 4. 2-Cyclopentenone, 2-Mehtyl-2-cyclopentenone, 5. 1,2-Dimethoxy-benzene, 1,4-Dimethoxy-2-methyl-benzene. Solid Products: Biochar, Coke Gas Products: CO_2, CO, H_2O, H_2	[119]
Corn Cob, Polyethylene	500°C-600°C	1. GC for gaseous products 2. GC/MS for liquid products	-	1. Liquid 2. Gas 3. Solid	Gas Products: CO, CO_2, CH_4, H_2 Liquid Products: Phenols, Alcohols, Acids, Esters, Ethers & Ketones. Solid products: Biochar	[120]
Chlorella vulgaris, Nano-chloropsis oceanica, Arthrospira plentesis (Microalgal Species)	450, 550, 650°C	1. Py-GC, GC/Q-TOF MS technique analyzed the complex mixture of volatile products	-	1. Gas & condensable vapors 2. Solid	Gas & Liquid Products: Alcohols, Carboxylic Acids, Esters, Furans Phenols, Esters.: Nitrogen containing Compounds (Amides, Nitriles, Pyrroles/Indoles)	[118]

Corn Stover	350-650℃	1. GC-MS for semi-quantitative analysis 2. GC for non-condensable gases analysis 3. Karl Fischer Titration for analyze water in Bio-oil.	-	1. Liquid (Bio-oil) 2. Gas (non-condensable) 3. Solid (Biochar)	Liquid Products: Acetone, Hydroxy-acetone, 2-Butanone, Cyclopentanone, Dimethyl-cyclopentenone, Phenol, P-cresol, 4-Ethylephenol, Methanol. Gas Products: CO, CO_2, CH_4, H_2, $C_2 - C_4$ hydrocarbon	[121]
Wheat straw and pine sawdust	30-900℃	1. TGA for mass loss 2. FTIR for real-time analysis of evolved gases 3. GC/MS for detailed identification of condensable vapors.	-	1. Gas (non-condensable) 2. Liquid (condensable) 3. Solid (char)	Gas Products: CO, CO_2, CH_4 Liquid Products: Cyclohexene-3,5-diol, pyrazole, 1,4 -dimethyl-cyclo-pentane-thiol, Furfural, 3-methyl-phenol, 2,4-Dimethyl-phenol, 1-Ethoxy-4-methyl-benzene.	[123]
Cellulose, wood, cow manure, poultry manure, saw dust blend, pine wood chips, wheat straw, grass.	300-700℃	1. Ultimate/Elemental analysis 2. Proximate Analysis 3. Stability Test	1. Gases CO, CO_2, CH_4, H_2 2. Volatile Mix from Wood 3. Volatile mix from wood 4. Apparent Loss Composition	1. Solid Biochar 2. Gas 3. Bio-oil	Solid Products: 1. Biochar Gas Products: 1. CO, CO_2, CH_4, H_2 Liquid Products: 1. Aromatic Hydrocarbon structure	[108]